T7 DNA polymerase treatment improves quantitative sequencing of both double-stranded and single-stranded DNA viruses

Maud Billaud[1], Ilias Theodorou[1,3], Quentin Lamy-Besnier[1], Shiraz A. Shah[4], François Lecointe[1], Luisa De Sordi[2,3], Marianne De Paepe[1] and Marie-Agnès Petit[1*]

1. Université Paris-Saclay, INRAE, Micalis unit, Jouy en Josas France
2. Sorbonne Université, INSERM, Centre de Recherche St Antoine, Paris, France
3. Paris Center for Microbiome Medicine (PaCeMM) FHU, AP-HP, Paris, France.
4. Copenhagen Prospective Studies on Asthma in Childhood, Copenhagen University Hospital, Herlev-Gentofte, Ledreborg Allé 34, DK-2820 Gentofte, Denmark

*Corresponding author, marie-agnes.petit@inrae.fr

Summary

Background: Bulk microbiome, as well as virome-enriched shotgun sequencing only reveals the double-stranded DNA (dsDNA) content of a given sample, unless specific treatments are applied. However, genomes of viruses often consist of a circular single-stranded DNA (ssDNA) molecule. Pre-treatment and amplification of DNA using the multiple displacement amplification (MDA) method enables conversion of ssDNA to dsDNA, but this process can lead to over-representation of these circular ssDNA genomes. A more recent alternative permits to bypass the amplification step, as library adapters are ligated to sheared and denatured DNA, after an end-modification step (xGen kit). However, the sonication step might shear ssDNA more efficiently than dsDNA, therefore introducing another bias in virome sequencing. These limitations prompted us to explore an alternative method of DNA preparation for sequencing mixed ssDNA and dsDNA viromes.

Results: Using a synthetic mix of viral particles, we made use of the T7 DNA polymerase (T7pol) to convert viral circular ssDNA molecules to dsDNA, while preventing over-replication of such molecules, as is the case with the Phi29 DNA polymerase. Our findings indicate that using T7pol and a mix of degenerated primers to convert ssDNA to dsDNA prior library preparation is a good alternative to the currently used methods. It better represents the original synthetic mixtures compared to MDA or direct application of the xGen kit. Furthermore, when applied to two complex virome samples, the T7pol treatment improved both the richness and abundance in the *Microviridae* fraction.

Conclusion: We conclude that T7pol pretreatment is preferable to MDA for the shotgun sequencing of viromes, which is easy to implement and inexpensive.

Keywords:

T7 DNA polymerase, shotgun sequencing, single-stranded DNA

49 ***Background***

50 In the last ten years, many methodological improvements have helped generate informative
51 metagenomics datasets for the virus-enriched fraction (or virome) of any type of environmental or
52 biological sample (Castro-Mejia et al., 2015; Deng et al., 2019; Hsieh et al., 2021; Shkoporov et al.,
53 2018; Wang et al., 2022). A particular difficulty of virome sequencing lies in the fact that the genetic
54 material of viruses is not exclusively made of double-stranded (ds) DNA, as is the case for bacteria and
55 higher organisms. It is frequently composed of single-stranded (ss) DNA and ss- or dsRNA. To our
56 knowledge, a single method allowing the preparation of all these substrates at once for deep
57 sequencing is not yet available. Even the simpler challenge of disposing of a method for the sequencing
58 of both ds and ssDNA viruses is not completely solved.

59 Initially, most viromes were sequenced after a multiple displacement amplification (MDA) step, which
60 was a convenient way to increase the usually low amounts of viral DNA to quantities compatible with
61 library preparation. It became rapidly obvious that MDA introduced a bias favoring small and circular
62 ssDNA viral genomes (the smallest ssDNA genomes are approximately 2000 nt long, while larger
63 inoviruses are approximately 7000 nt long) (Kim and Bae, 2011; Yilmaz et al., 2010). This is because the
64 Phi29 DNA polymerase used for MDA has potent strand displacement activity (Blanco et al., 1989).
65 Therefore, once these small ssDNA genomes are converted into dsDNA, the polymerase proceeds for
66 further rounds, generating long concatemers. Tests with synthetic mixes of viral genomes
67 unambiguously demonstrated this caveat of MDA for mixes of ss- and dsDNA genomes (Roux et al.,
68 2016).

69 Two main solutions were proposed to circumvent this problem. First, the "short MDA (sMDA)" method
70 consisted of reducing the incubation time of the MDA treatment from the normally recommended 90-
71 120 minutes to 30 minutes (Deng et al., 2019). The second solution consisted of replacing the
72 amplification step with a library kit able to add adapters to ssDNA molecules. Here, after an initial
73 shearing step, all DNA molecule extremities, both ss- and dsDNA, receive a short extension using an
74 "adaptase", the nature of which is kept secret by the manufacturer. Then, an additional linker is added,
75 allowing PCR amplification and sample labeling. This methodology is used in the Accel-NGS kit from
76 Swift Biosciences (recently acquired by Integrated DNA Technologies (IDT) and rebranded as the xGen
77 kit, below xGen). It was initially developed for the sequencing of ancient DNA, and has started to be
78 used in the virome community (Roux et al., 2016). For this second method, tests with synthetic mixes
79 showed that the bias in favor of ssDNA viruses was significantly reduced (Roux et al., 2016).

80 Using the xGen kit also comes with a drawback: the DNA shearing step is performed before the
81 conversion of ssDNA to dsDNA, which may result in discrepancies if ssDNA is more readily sheared than
82 dsDNA. This leads to possible downstream biases in library preparations, which require a
83 homogeneous size distribution of the DNA fragments.

84 This prompted us to search for an alternative method of DNA preparation for the sequencing of
85 mixed ssDNA and dsDNA viromes. We present here this new method based on the use of T7 DNA
86 polymerase (T7pol) and compare it to two other methods: sMDA amplification, or no pretreatment.
87 Then, all libraries were prepared with the xGen kit, for comparison purposes. We first compared the
88 performance of the three methods on a synthetic community of five phages, and then tested the
89 new T7Pol pre-treatment method followed by xGen libraries on two human viromes, in comparison
90 with samples that had not been pre-treated.

91

92

Methods

DNA, enzymes, oligonucleotides, kits and other materials

ssDNA of M13mp18 and PhiX174, as well as dsDNA of PhiX174, were purchased from New England Biolabs (NEB, references N4040S, N3023L and N3021S, respectively). T7pol was purchased from NEB (ref. M0274) and used following the manufacturer's instructions. Turbo DNAse I was purchased from Thermo Fisher Scientific (reference AM2222), and benzonase from Millipore (purity > 90%, reference 70746). For MDA treatments, the Genomiphi2 kit was purchased from Fisher Scientific (reference 10628505). The "xGen ssDNA Low-Input DNA Lib Prep 16rxn" (previously, Accel NGS S2 kit) was purchased from IDT (reference 10009859). Random oligonucleotides of a 20-nt size were purchased from Eurofins Genomics. SPRI Select magnetic beads were purchased from Beckman Coulter (reference B23318). To filter out bacteria from lysates and samples, polyethersulfone (PES) syringe filters 0.8/0.2 µm were used (Pall corporation, reference 4187).

Phage lysates preparations

Two *Escherichia coli* infecting phages with ssDNA genomes were selected for the study: PhiX174 and an M13 derivative. PhiX174 is a *Microviridae* that forms a tail-less icosaedric capsid enclosing its circular 5386 nt ssDNA genome. It was grown on *E. coli* strain C, which codes for its appropriate core LPS receptor (Feige and Stirm, 1976). M13-yfp (De Paepe et al., 2010) is a filamentous phage of the *Inoviridae* family harboring a 7916 nt long circular ssDNA genome. It was grown on *E. coli* strain MG1655 F'kanR, a strain coding for the F pilus, which is the M13 receptor. Three dsDNA Caudoviricetes were also selected for the study: SPP1, T4 and lambda. T4 and lambda are *Escherichia coli*-infecting phages and were grown on *E. coli* strain MG1655. Inside the virions, the T4 genome is a 169 kb-long, linear dsDNA molecule, while the lambda linear genome has a shorter, 48 kb-long linear dsDNA genome. Finally, the *Bacillus subtilis* infecting phage SPP1 was propagated on strain YP886, generating virions containing a linear, 46 kb-long genome.

Phage lysates of T4, SPP1, lambda and phiX174 were prepared as described previously (Sausset et al., 2022), and bacterial remains were removed by centrifugation (5000 g, 7 min, 4°C), followed by filtration through PES filters. A lysate of M13-yfp was obtained by propagating the infected strain in 50 mL of LB-broth Lennox (Formedium) with 50 µg/mL kanamycin up to OD_{600} 1, removing bacteria by centrifugation (5000 g, 7 min, 4°C), and filtering the supernatant with PES filter. Stocks were kept at 4°C in salt-magnesium (SM) buffer (200 mM NaCl, 50 mM Tris pH 7.5, 10 mM $MgSO_4$).

Pure phage DNA preparation

From lysates, phages were concentrated by overnight centrifugation (20 000 g, 16 h), resuspended in 0.5 mL SM buffer, and loaded on SM-iodixanol gradients as described (Sausset et al., 2022). The phage-containing fraction was dialyzed against SM buffer and stored at 4°C. Prior to phage DNA extraction, purified particles were treated for 1 h at 37°C with DNaseI (8 units) and RNaseA (20 units) in SM buffer complemented with 0.5 mM $CaCl_2$ to eliminate any residual bacterial DNA or RNA. The reaction was stopped by adding EDTA (20 mM).

To extract DNA from the capsids, samples were then treated with proteinase K (2 mg/mL) and SDS (0.5%) for 20 min at 56°C. Phage DNA was then extracted by phenol–chloroform-isoamyl alcohol (25:24:1) extraction followed by two chloroform-isoamyl alcohol (24:1) purification steps. At each step, the solvent and aqueous phases were separated by centrifugation 15 minutes at 12 000g, 4°C. DNA was then supplemented with 300 mM potassium acetate pH 4.8, and precipitated with two volumes of ethanol, centrifuged for 30 min at 12000 g and 4°C, and the pellet was resuspended in 10 mM Tris buffer pH 8. Phage dsDNA concentration was estimated using a Qubit device.

137 *Phage quantification and preparation of the synthetic phage mixes*

138 To prepare mixes containing phages in known concentrations, phage genome quantities of T4, lambda,
139 SPP1 and PhiX174 were determined by qPCR, in comparison to dilutions of pure DNA standards. For
140 these standards, concentration of PhiX174 ssDNA (from NEB) was verified both with a
141 spectrophotometer (Nanodrop) and with a fluorescent-based method (Qubit). For M13 and PhiX174
142 ssDNA, Qubit values were 16 to 27% lower than Nanodrop values, respectively. Nanodrop values were
143 kept, as they were closer to the Supplier's indication (supplementary table 1) . For dsDNA qPCR
144 standards, highly purified phage stocks of T4, SPP1 and lambda were prepared and quantified as
145 described in the "Pure phage DNA preparation" section. Next, each stock of pure DNA was diluted in
146 10 mM Tris pH 8 to obtain a concentration of $5x10^6$ phage genomes in 6 µL. The samples were further
147 diluted four times by 3-fold dilution steps, to obtain the calibration range ($1.8x10^5$ to $5x10^6$ genomes),
148 and aliquots stored at -20°C until use.
149 Before quantifying the four phage lysates, they were treated with DNaseI using 1 µL of enzyme/ml
150 phage sample (1 h at 37°C) to eliminate any residual free DNA, and then treated at 95°C for 5 minutes,
151 for capsid denaturation. Primers indicated in supplementary table 2 were used at a concentration of
152 200 nM. Three dilutions of each heat-denatured phage stock were compared to the calibration curves
153 of highly purified DNA of the corresponding phage, as described above. qPCR was performed in a total
154 volume of 15 µL (6 µL purified DNA or phage particle dilution and 9 µL of amplification mix) in
155 MicroAmp Fast Optical 96-well plates sealed with MicroAmp Optical Adhesive Film (both from Applied
156 Biosystems, reference 4346906 and 4311971, respectively) using the Luna universal qPCR master mix
157 (NEB, ref M3003). Amplifications were run in duplicate on a StepOnePlus real-time PCR system with
158 the following cycling conditions: 95°C for 5 min, (95°C for 15 s, 58°C for 45 s, 72°C for 30 s) for 45 cycles,
159 72°C for 5 min, 95°C for 15 s, 60°C for 15 s, and 95°C for 15 s. The analysis of the melting curves
160 confirmed the specificity of the primers. Data analysis was performed with StepOne software 2.3.
161
162 The M13-yfp lysate could not be quantified by qPCR due to coat resistance to heat (González-Cansino
163 et al., 2019), so it was quantified by plaque formation units on the MG1655 F'kan strain. Plaque counts
164 of M13-yfp were easy to determine, as it is an M13mp18 derivative making much clearer plaques than
165 the parental M13. Once each phage stock had been quantified, synthetic mixes were prepared. Initial
166 phage concentrations in each stock, as well as volumes added to compose each mix, are presented in
167 supplementary table 3.
168
169 *Synthetic mixes DNA extractions*

170 To extract the DNA from the two synthetic mixes, an initial volume of 500 µL was used and DNA was
171 extracted by phenol-chloroform treatment, as described in the "pure phage DNA preparation"
172 section., resuspended in 25 µL of 10 mM Tris (pH 8), and dispatched twice for the three treatments as
173 follows: 1 µL for MDA pretreatment (according to the Genomiphi2 kit instructions), 5 µL for T7pol
174 pretreatment, and 5 µL for the xGen library without pretreatment. Final DNA yields were in average
175 100 ng for untreated and T7pol treated samples, 25 ng for the Genomiphi amplified mix with low
176 proportion of ssDNA, and 500 ng for the Genomiphi amplified mix with high proportion of ssDNA.

177
178 *T7pol pretreatment*
179
180 Primers for T7pol priming should have a minimum length of 15 nt (Hernandez et al., 2016), and their
181 optimal size is 21 nt (C.C. Richardson, personal communication). To test whether degenerated primers
182 could be used with T7pol to convert any phage ssDNA to dsDNA, degenerated primers of 20 nt were
183 tested on ssDNA from PhiX174 and M13mp18. For the annealing step, samples containing 250 ng of
184 M13mp18 and 250 ng of PhiX174 ssDNA in a final volume of 25 µL of water were incubated with varying
185 concentrations of oligonucleotides for 5 minutes at 65°C (primer concentrations are indicated at this
186 first annealing step, samples are then diluted 2-fold for the replication step). The samples were then

187 allowed to cool down slowly by disposing them on floaters over a beaker containing 25 mL of 65°C
188 water and placed at room temperature until final temperature was below 46°C (usually 10 minutes).
189 Replication was then initiated by adding 300 µM dNTPs, 1X T7pol buffer, 50 µg/mL BSA and 5 units of
190 T7pol in each tube completed with water to a final volume of 50 µL, followed by incubation for 5
191 minutes at 37°C. Reactions were stopped by placing the samples at 75°C for 20 minutes. Prior gel
192 loading, samples were adjusted to 0.2% SDS, 10 mM EDTA and 0.5 mg/mL proteinase K, and incubated
193 at 50°C for 30 minutes, to remove proteins that might prevent proper migration of the DNA molecules.
194 Products (15 µL) were separated on a 0.7% agarose gel containing 40 µg/mL ethidium bromide. For
195 the T7pol pretreatment of phage DNA mixes, the same conditions were applied, except that
196 degenerated primers were used at a final concentration of 10 µM, together with 5 µL of DNA mix
197 complemented with water to a final volume of 25 µL. The next replication step was performed in a
198 final volume of 50 µL with 5 units of T7pol.
199
200 *Effect of sonication and magnetic bead size selection on ss- and dsDNA*
201
202 PhiX174 ssDNA and dsDNA were each diluted at 20 ng/µL into 100 µL volumes and treated for
203 sonication using conditions applied for library preparation (see below). Half of each sample was then
204 submitted to SPRIselect magnetic bead binding, using conditions removing dsDNA fragments below
205 200 bp, as applied for library preparation (see below), except that elution was done in the same 50 µL
206 volume of Tris 10 mM pH 8. To visualize ssDNA fragment sizes, products were then separated on a 10
207 cm-long polyacrylamide denaturing gel (5% of acryl/bis 19:1, 8 M urea, 1 x TBE). For this, 10 µL of
208 formamide stained with bromophenol blue was added to 10 µL of each sample, incubated at 90°C for
209 5 minutes, and then placed on ice. Samples (20 µL) were then loaded on a preheated gel (>1 hour
210 migration, 450 volts) and separated for ~20 minutes at 300 volts until bromophenol blue reached the
211 gel border. The gel was stained for 30 minutes with Syber Gold (Invitrogen, reference S11494, 1X final
212 concentration), and bands were revealed by a Bio-Rad ChemiDocTM MP imaging system. The size at
213 the maximum signal intensity of each smear was estimated with Image Lab software (Bio-Rad
214 Laboratories). Six PCR fragments 601, 440, 330, 279, 200 and 116 bp-long were denatured with
215 formamide and run as a size ladder.
216
217 *Library preparations, synthetic phage mix sequencing and analysis*
218
219 DNA preparations from the synthetic phage mixes were first pretreated (or not) for the conversion of
220 ssDNA to dsDNA using either the Phi29 polymerase of the Genomiphi2 kit according to the supplier's
221 instructions with a 30-minute incubation or T7pol (see Results section). Next, all samples were
222 sonicated (100 µL in 1.5 mL tubes) with a Diagenode Bioruptor Pico device in a cooled water bath (4°C)
223 for 21 sec with 90 sec breaks for 3 cycles, centrifuged to collect droplets on the side of the tubes, and
224 sonicated again for 21 sec with 90 sec breaks for 2 cycles to generate DNA segments of an average size
225 of approximately 500 bp. DNA samples were then concentrated to 20 µL using SPRIselect magnetic
226 beads from Beckman Coulter (ratio beads/DNA=1.2) to remove fragments below 200 bp. All samples
227 were then processed for library preparation using the xGen kit, following the manufacturer's
228 instructions. These library steps included (1) adaptase (37°C, 15 min then 95°C, 2 min); (2) extension
229 (98°C, 30 s; 63°C, 15 s; 68°C, 5 min); (3) magnetic bead cleaning; (4) linker ligation (25°C, 15 min); (5)
230 magnetic bead cleaning; (6) DNA concentration estimation by Qubit (high sensitivity kit); and (7)
231 indexing by PCR (98°C, 30 s followed by 4 to 14 cycles of 98°C, 10 s; 60°C, 30 s; 68°C, 60 s) depending
232 on the initial DNA concentration.
233
234 Paired-end sequencing (2x150 nt) was performed on an Illumina ISeq100 system at a depth of 800 000
235 reads per sample. Read cleaning was then computed with fastp (v 0.23.1, (Chen et al., 2018)) using the
236 following parameters: --trimfront2 15 --trimtail1 2 --trimtail2 2 –trim_poly_g –trim_poly_x –r –W 4 –
237 M 20 –u 30 –e 20 –l 100 –p –w 12. These parameters were used to remove the adapters present at
238 read extremities with xGen libraries. Read mapping of both paired and unpaired reads on the phage
239 genomes was then conducted with bwa (Li and Durbin, 2009) and the –a parameter. Next, the data

were treated and analyzed with msamtools and the following parameters: msamtools filter –b –u –l 80 –p 95 –z 80 –besthit –S and then msamtools profile –multi=proportional. The number of reads mapped per genome was normalized in relative abundance (rel) at the msamtools profile step using the default parameter. Rel are computed as follows: an "abundance" value of each genome is estimated by the number of reads mapped to that genome, divided by its length and normalized by the sum of abundances across all five genomes. The proportion of each phage within the sequenced sample was then estimated by this rel ratio.

To compare final compositions of the sequenced mixes, Aitchison distances were used. This distance is a Euclidean distance based on centered log ratio (CLR) transformations of a virus count matrix. CLR transformation accounts for the compositionality that is especially pronounced when only a few taxa are present. In such cases Aitchison distances provide the most accurate metric for gauging the similarity of samples.

Human fecal virome sample preparation and treatment

Fecal samples (0.2 g) from two healthy donors S4 and S18 were first resuspended in 4 mL of 10 mM Tris, pH 7.5, and then centrifuged (5 200 g, 30 min, 4°C). The supernatant was filtered using 0.2 µm diameter PES filters. Then, a benzonase-nuclease treatment (75 U per sample) was performed for 2 h at 37°C. The viral samples were then concentrated by precipitation overnight at 4°C using polyethyleneglycol (PEG 8000, 10% w/v) and NaCl 0.5 M. After centrifugation (5 200 g, 1 h, 4°C), the pellet was retrieved and processed for DNA extraction as described in the "Pure phage DNA preparation" section. Each DNA sample was then divided into two parts: one was kept unprocessed, and the other was further treated with T7pol as described above. All samples libraries were then prepared with the xGen kit. Paired-end sequencing (2x150 nt) was performed on an Illumina platform at a depth of 5 million read pairs per sample.

Bioinformatics analysis of the virome samples

The different steps of the analysis are summarized in supplementary figure 1. First, reads were cleaned with fastp as described for the synthetic mix sequencing, above. To remove contamination, all the reads mapping to the human genome (GRCh38) according to Bowtie2 (v 2.4.1, (Langmead and Salzberg, 2012)) with the --very-sensitive option were then excluded. The remaining reads were assembled using SPAdes (options --only assembler -k 21,33,55,77,99,127, v 3.15.3, (Prjibelski et al., 2020)). Deduplication of contigs at the species level (95% average nucleotide identity) was performed using BLAT (Kent, 2002) as previously published (Shah et al., 2023). Viral contigs were identified through two parallel approaches: using softwares and searching by alignment against Refseq, as well as recently released phage gut databases. For the software, VirSorter2 (options --include-groups dsDNAphage,NCLDV,RNA,ssDNA,lavidaviridae --exclude-lt2gene --min-length 2000 --viral-gene-required --hallmark-required --min-score 0.9 --high-confidence-only, v 2.2.3, (Guo et al., 2021), VIBRANT (default parameters, v 1.2.1, (Kieft et al., 2020)), and CheckV (v 0.8.1, database v 1.5, (Nayfach et al., 2021a)) were used. For CheckV, only the contigs with a minimum of "medium" quality were considered viral. Contigs classified as viral by any of these three softwares (with the mentioned parameters) were kept. For the databases, contigs were aligned using BLAT (v 36, (Kent, 2002)) against the following databases: COPSAC (Shah et al., 2023), GVD (Gregory et al., 2020), MGV (Nayfach et al., 2021b), GPD (Camarillo-Guerrero et al., 2021) and viral RefSeq. The contigs that aligned against any contig in the databases with an alignment length >= 80% of the database contig were considered viral. A list of unique viral OTUs was generated by combining the outputs of both of these approaches. Gene calling on viral contigs was performed with Prodigal (Hyatt et al., 2010). *Microviridae* were identified among all these viral contigs by searching for the presence of either the major capsid protein (MCP) or replication initiation protein (Rep). For this, we ran HHsearch (Soding, 2005) against specific PHROGs

288 profiles (PHROG 514 for the MCP, and PHROGs 713 and 942 for Rep), and retained hits with at least
289 90% probability and 60% coverage of the target protein (Terzian et al., 2021). To retrieve a closer
290 relative for the identified *Microviridae*, a vContact2 graph was constructed (Bin Jang et al., 2019),
291 which included these contigs and INPHARED (March 2023 version) as reference database (Cook et al.,
292 2021). This graph was then analyzed with graphanalyzer (Pandolfo et al., 2022). For comparison
293 purposes, the four samples were then subsampled to 2 M paired-end reads per sample using seqtk (v
294 1.3, https://github.com/lh3/seqtk). The subsampled reads were then aligned against the set of viral
295 contigs using BWA-mem2 (v 2.2.1, (Vasimuddin et al., 2019)) with the -a option. Then, using
296 msamtools, reads were first filtered to only keep alignments > 80 bp with >95% identity over >80%
297 read length and only keeping the best alignment for each read (options -l 80 -p 95 -z 80 –besthit). To
298 exclusively work with contigs for which there is sufficient support of its presence in a given sample,
299 only contigs for which the overall sequencing depth was >= 1 and at least 50% of the contig length was
300 covered were kept (values computed using msamtools coverage –summary command). The relative
301 abundance of each contig passing these criteria was determined by using the msamtools profile
302 (options --multi=proportional --unit=rel). At the end of these treatments, sample S4 contained 269
303 viral OTUs when no T7pol treatment had been applied, and 181 viral OTU for the T7pol pretreatment
304 sample. Sample S18 was richer, with 645 and 702 vOTU without and with T7pol treatment,
305 respectively. Those relative abundances were finally analyzed using the R package phyloseq (v 1.38.0,
306 (McMurdie and Holmes, 2013)).

307

308 ***Results***

309 *Comparing the fate of ssDNA and dsDNA during library preparations*

310 A necessary step of library preparations involves the production of DNA fragments of a homogeneous
311 size, either by enzymatic treatment or ultrasonic DNA shearing. Enzymatic treatment cannot target
312 ssDNA, and ssDNA treatment by sonication may result in systematic lower sizes compared to dsDNA.
313 Indeed, the xGen protocol mentions that fragmentation of ssDNA may result in shorter fragments and
314 lower library yields. To quantify this difference, samples of dsDNA and ssDNA corresponding to the RF1
315 replicating form and the virion form of the phage PhiX174 genome, respectively, were sonicated in
316 parallel (replicates performed on two different days) for the duration applied during library
317 preparation and separated on a urea-denaturing 5% acrylamide gel. After sonication, a lower size of
318 DNA strands was systematically observed for the ssDNA samples compared to the dsDNA samples
319 (peak size at 316 versus 562 nt for replicate 1 and 235 versus 330 nt for replicate 2, Figure 1: ds and ss
320 slots).

321 Some protocols concentrate the sonicated aliquots to 20 µL using magnetic beads for the adaptase
322 step of the xGen kit (see Methods). We tested whether ssDNA fragments were preferentially lost at
323 this step as well. Using the PhiX174 sonicated samples, total DNA recovery after the bead cleaning step
324 was estimated with a Nanodrop apparatus. Whereas a total loss of 42-48% relative to input DNA was
325 found for the dsDNA samples, this loss was more pronounced for ssDNA samples (74-84%). Migration
326 of these samples next to their untreated controls on the denaturing gel indicated that this preferential
327 loss was due to a higher size cutoff for ssDNA, compared to dsDNA, as the size at peak intensity
328 increased after bead treatment for ssDNA (from 316 to 407 nt in replicate 1 and from 235 to 325 nt in
329 replicate 2, Figure 1: ss and ssB labels), unlike for dsDNA (Figure 1: ds and dsB labels).

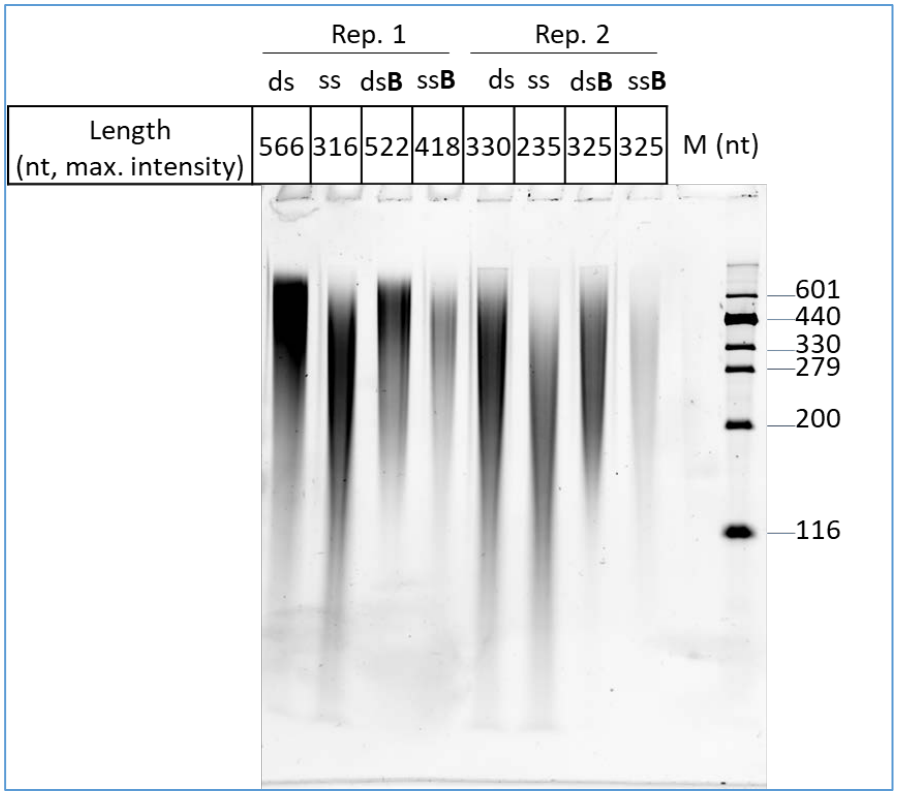

Figure 1. Effect of sonication and SPRI magnetic beads on ssDNA (ss slots) and dsDNA (ds slots) of PhiX174. All samples were sonicated for 5 cycles of 21 seconds, and a half volume was then treated with SPRI magnetic beads (B slots) to remove fragments below 200 bp. Samples were separated on a 5% acrylamide urea-denaturing gel. M: size marker. See the original gel picture in supplementary figure 2.

330 We concluded that both sonication and magnetic bead treatments had differential effects on ss- and
331 dsDNA, with ssDNA being cut to 56-71% of the average size of dsDNA and small fragment removal by
332 magnetic beads leading to a 2-fold lower recovery of ssDNA fragments compared to dsDNA.

333 *Setting up a ssDNA-to-dsDNA conversion protocol using T7 DNA polymerase.*

334 To limit any bias in the treatments of ss- versus dsDNA molecules, we therefore searched for a
335 quantitative method to convert ssDNA molecules to dsDNA prior to sonication. Contrary to the Phi29
336 DNA polymerase, T7pol has no intrinsic strand displacement activity, and does not open up the DNA
337 strands ahead of polymerization process (Blanco et al., 1989; Canceill et al., 1999; Lechner and
338 Richardson, 1983) (Figure 2A). Instead, a separate, replicative DNA helicase is responsible for this step,
339 as in most living organisms (Canceill et al., 1999). As a consequence, once a first round of replication

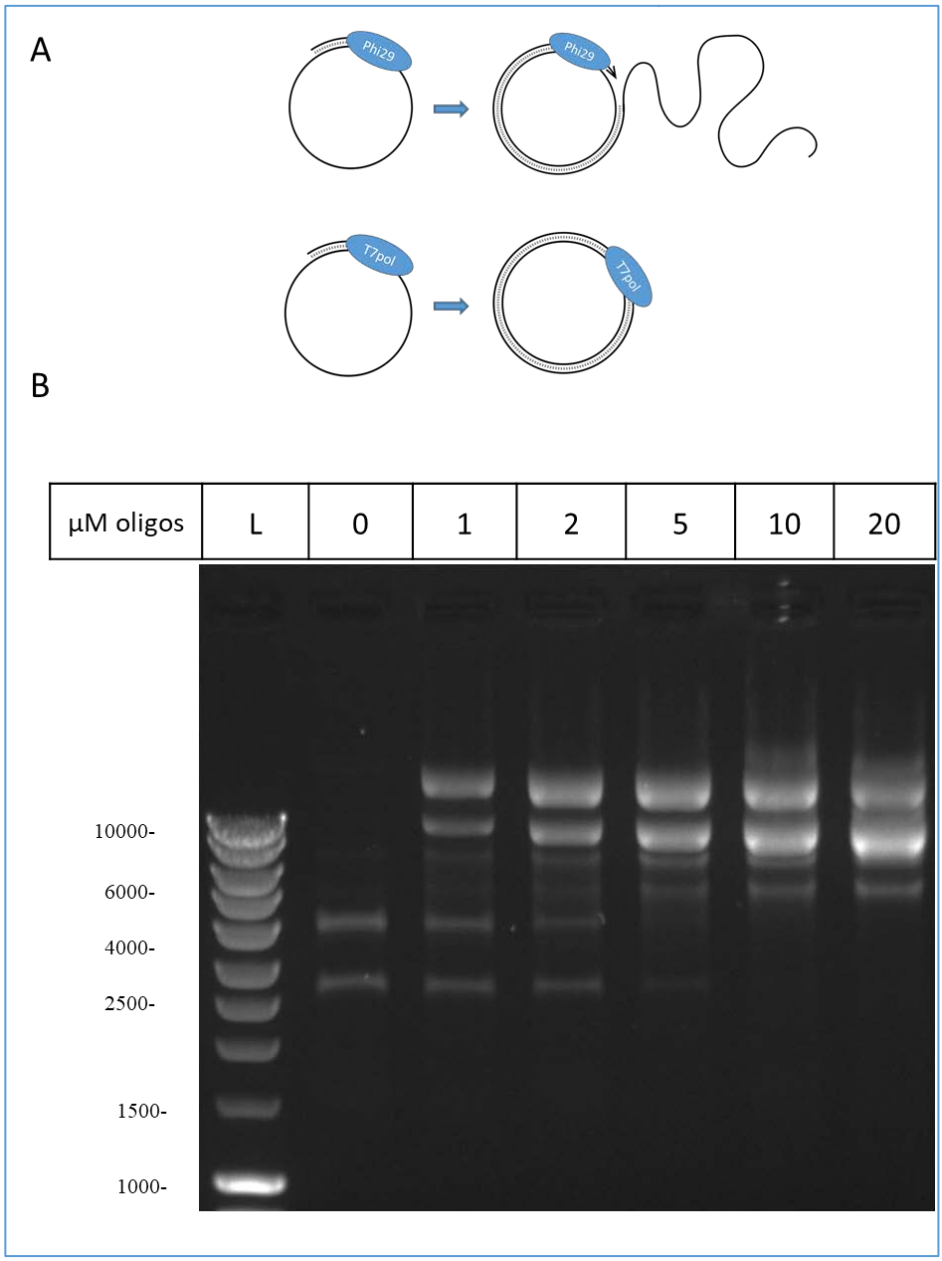

Figure 2: A. The different strand displacement activities of Phi29 DNA polymerase (up, rolling circle) and T7pol (down, stops after one round). B. Adjusting primer concentrations for T7pol conversion of ssDNA to dsDNA of M13 and PhiX174. Degenerated oligonucleotides (20 nt) were annealed at the indicated concentrations on a mix of M13 and PhiX174 ssDNA and incubated in the presence of T7pol. Products separated on 0.7% agarose gel are shown. Sizes (bp) of linear dsDNA standards (lane L, Smart ladder, Eurogentec) are indicated on the left (bp). See the original gel picture in supplementary figure 3.

340 has been completed on a circular ssDNA molecule, T7pol stops and unloads, therefore preventing DNA
341 overamplification.

342 To test conditions allowing T7pol replication initiation using degenerated oligonucleotides as primers,
343 a 1:1 weight mix of PhiX174 and M13mp18 circular ssDNA molecules was used (10 µg/mL final DNA
344 concentration). A range of oligonucleotide concentrations from 1 to 20 µM was tested, and repeated
345 three times. A representative gel is shown Figure 2B. We found that 10 µM of 20 nt long degenerated
346 oligonucleotides were sufficient to convert all the ssDNA species into dsDNA. In addition, and as
347 expected, no smear indicative of further rounds of replication beyond the first one was detected. The
348 marked intensity of the dsDNA bands, relative to ssDNA, was due to the higher affinity of ethidium
349 bromide for dsDNA.

350 We concluded that T7pol treatment of circular and ssDNA should be an efficient and quantitative way
351 to convert all DNA molecules to dsDNA prior to library preparation.

352 *A T7pol pretreatment of synthetic viromes generates more accurate results*

353 We therefore proceeded to test this T7pol treatment on mock phage mixes and compared it to other
354 ways of treating DNA for library preparation. For this, two synthetic mixes were prepared from stocks
355 of five phages, two of which were ssDNA phages (M13-yfp and PhiX174), and three dsDNA phages (T4,
356 lambda and SPP1). One mix contained 48.4% of ssDNA phage genomes (45.3% of M13-yfp, 3.1% of

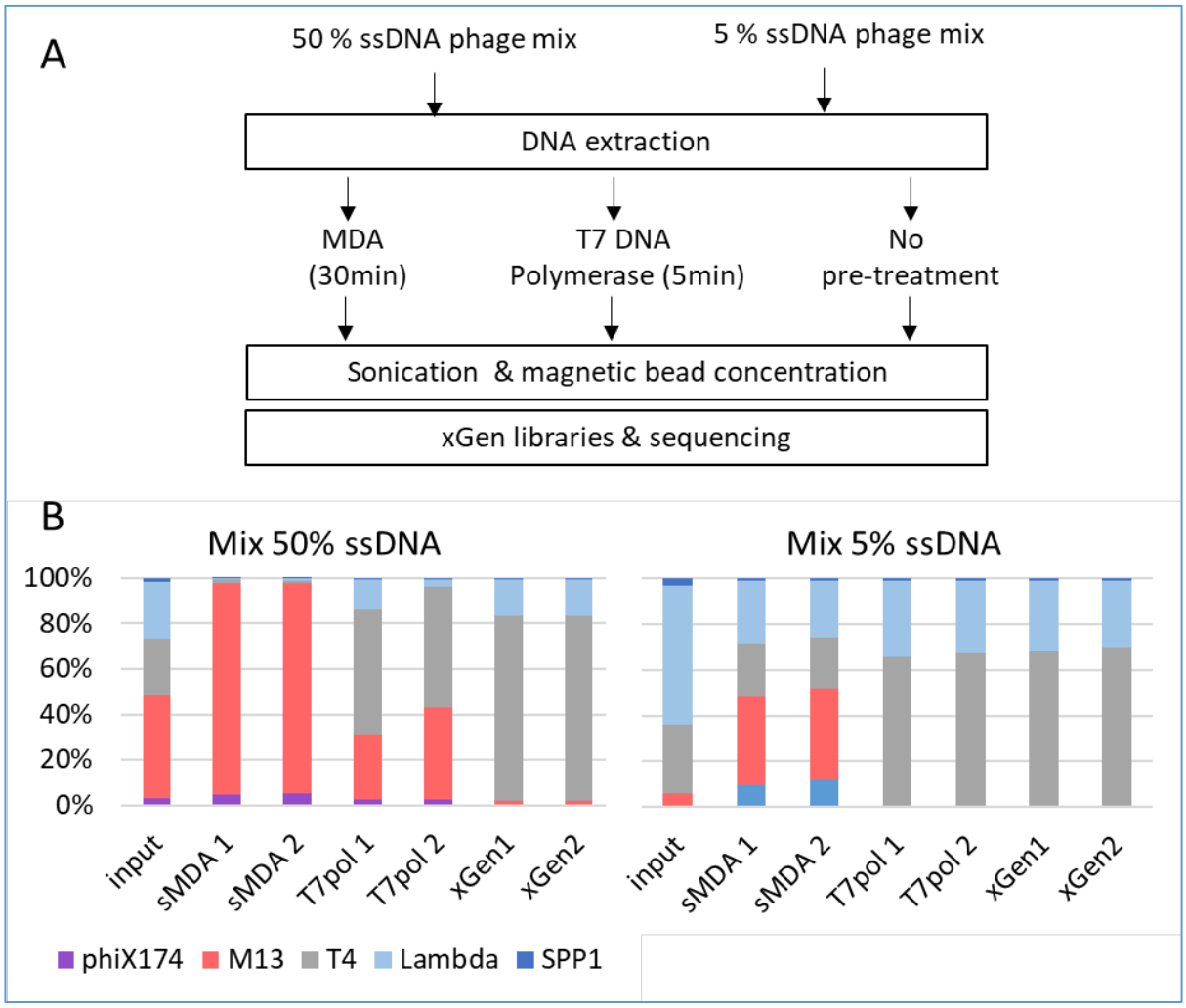

Figure 3. A: Comparison of protocols for sequencing ss- and dsDNA mixes. B. Input bar: Theoretical initial proportions of the 5 phages. Next six bars: Observed proportions of the 5 phages after deep sequencing (in duplicate, 1 and 2) of xGen DNA libraries either pre-treated with sMDA, T7pol, or without pre-treatment (xGen). Relative abundances are shown (rel values, see Methods).

357 PhiX174), while the other contained only 5.9% of ssDNA phage genomes (5.5% M13-yfp and 0.4%
358 PhiX174). The final and global phage concentration in each mix was approximately 10^9 genomes/mL to
359 mimic realistic viral concentrations in fecal samples (assuming a 10-fold dilution of fecal matter at 10^{10}
360 particles/g).

361 Next, DNA was extracted from the two mixes, and each was subjected to one of the three following
362 treatments (Figure 3A): (i) short MDA (sMDA), (ii) T7pol-dependent DNA replication using an excess of
363 10 µM degenerated oligonucleotides, and (iii) no pretreatment. Then, all samples were sonicated in a
364 final volume of 100 µL and concentrated using magnetic beads. Finally, all were processed with the
365 xGen kit for library preparation (see Methods for details). Each treatment was performed in duplicate,
366 and the 12 samples were then sequenced on an Illumina platform (127 000 to 2.7 million reads per
367 sample were obtained). Read mapping on the 5 phage genomes was converted into relative
368 abundances, to estimate the proportion of each phage in the mix at the end of all treatments and to
369 compare them to their theoretical initial ratio (Figure 3B, and supplementary table 4).

370 We found that the DNA samples treated directly with xGen libraries (absence of pretreatment) led to
371 a major depletion of the ssDNA phages: starting with the 48.4% input ssDNA mix, ssDNA phages only
372 contributed 1.8-1.9% of the final sequencing result. The reduction of the ssDNA mix was even more
373 drastic with 5.9% input ssDNA, as no reads matching the two ssDNA phages were obtained in one of
374 the replicates, and M13 contributed only 0.09% of the sequenced virome in the other experiment.
375 Since input DNA strands for library preparation were twice less abundant for ssDNA phages relative to
376 dsDNA phages, the overall ssDNA phage depletion was 10-fold for the high input mix and over 30-fold
377 for the low input mix.

378 With the short MDA pretreatment, starting with the 48.4% input ssDNA mix, 98% of ssDNA phage
379 genomes were recovered, and 48-52% were recovered when using the 5.9% input ssDNA mix (here
380 and below, no correction for single-strand molecules was applied, as all molecules were in the dsDNA
381 state for library preparation). We conclude that overamplification occurred in both cases by factors of
382 2 and 8.6, respectively.

383 Finally, the T7pol pretreatment gave a result that was more congruent with input DNA: for the 48.4%
384 ssDNA input mix, similar proportions (31-43%) of ssDNA phage were recovered, and 8.2-fold lower
385 ssDNA (0.7%) was found for the 5.9% input mix.

386 To quantify the congruence between the initial mix compositions and the different pretreatments
387 while accounting for the compositionality of the data, we computed Aitchison distances, a metric used
388 to compare ecosystem compositions (Aitchison, 1982). Distances obtained between each input DNA
389 mix and the various outputs, using the abundances from supplementary table 4, are reported in Table
390 1.

391 Table 1: A. Aitchison distances between the compositions obtained from the different pretreatments and the
392 input composition with low ssDNA amounts (5.9%). B. Same calculations for the high ssDNA input mix.

A.	Mix low ssDNA
xGen 1	8.17
xGen 2	5.97
sMDA 1	3.86
sMDA2	4.02
T7pol 1	2.29
T7pol 2	2.23

B.	Mix high ssDNA
xGen 1	3.72
xGen 2	3.93
sMDA 1	4.39
sMDA 2	4.34
T7pol 1	2.15
T7pol 2	2.31

393

394 T7pol pretreatment was more quantitative than both other methods, regardless of the input
395 ssDNA/dsDNA ratio. Among the two other methods, short MDA pretreatment was more quantitative
396 than direct xGen libraries for the mix with a low ssDNA concentration. However, the opposite was true
397 at higher ssDNA concentrations. As a reference, the distance between the two input mixes themselves
398 was also computed and found to be 3.05. This indicates that the T7pol pretreatment gave results closer
399 to its initial mix (a distance of approximately 2) than the distance between the two input stocks.

400 *T7pol treatment of two viromes*

401 To investigate the effect of T7pol treatment on complex environmental samples, two fecal samples
402 were collected from healthy individuals (S4 and S18). Viromes were prepared, DNA extracted, and each
403 sample was then treated or not with T7pol prior to sequencing, following the protocol described
404 above. xGen libraries were then prepared exactly as for the synthetic communities. Reads were
405 assembled de novo in contigs, which were then processed for the identification of viral ones
406 (supplementary table 5). Among them, *Microviridae* were recognized by the presence of either the
407 major capsid protein-encoding gene or the replication gene (see supplementary table 6 and
408 supplementary figure 5 for details on these contigs). Mapping back the reads on all viral contigs
409 allowed to determine the relative abundance of *Microviridae*. For the first S4 sample, the relative
410 abundance of *Microviridae* increased from 24% to 74% of all viral contigs upon T7pol treatment.
411 Richness in *Microviridae* also slightly increased, from 28 to 33 species. We noted, however, that 6 of
412 the *Microviridae* contigs detected in the untreated samples were not present in the T7pol sample,
413 while conversely, 11 *Microviridae* contigs were found only in the T7pol sample. A detailed analysis of
414 the *Microviridae* profile indicated that each microvirus contig gained some level of abundance (some
415 8 +/- 6-fold on average), as indicated in Figure 4A (see also supplementary table 7). For the second S18
416 sample, the relative abundance of microviral species among viral contigs increased from 25% to 30%,
417 and richness shifted from 5 to 8 species (Fig. 4B and supplementary table 7). We therefore conclude
418 that the T7pol treatment improves overall the detection of *Microviridae* in complex samples,
419 marginally in one case, and more substantially in the other case. Conversely, relative abundances of
420 dsDNA, Caudoviricetes contigs were reduced upon T7pol treatment in sample S4. Their abundance was
421 mostly unchanged in sample S18 (supplementary figure 4 and supplementary table 8). This was
422 expected, as these two categories represent most of the signal, and therefore mirror each other in
423 human fecal samples. We conclude that the T7pol treatment allows for better detection of ssDNA
424 phages in natural samples, in agreement with the results obtained for synthetic communities.

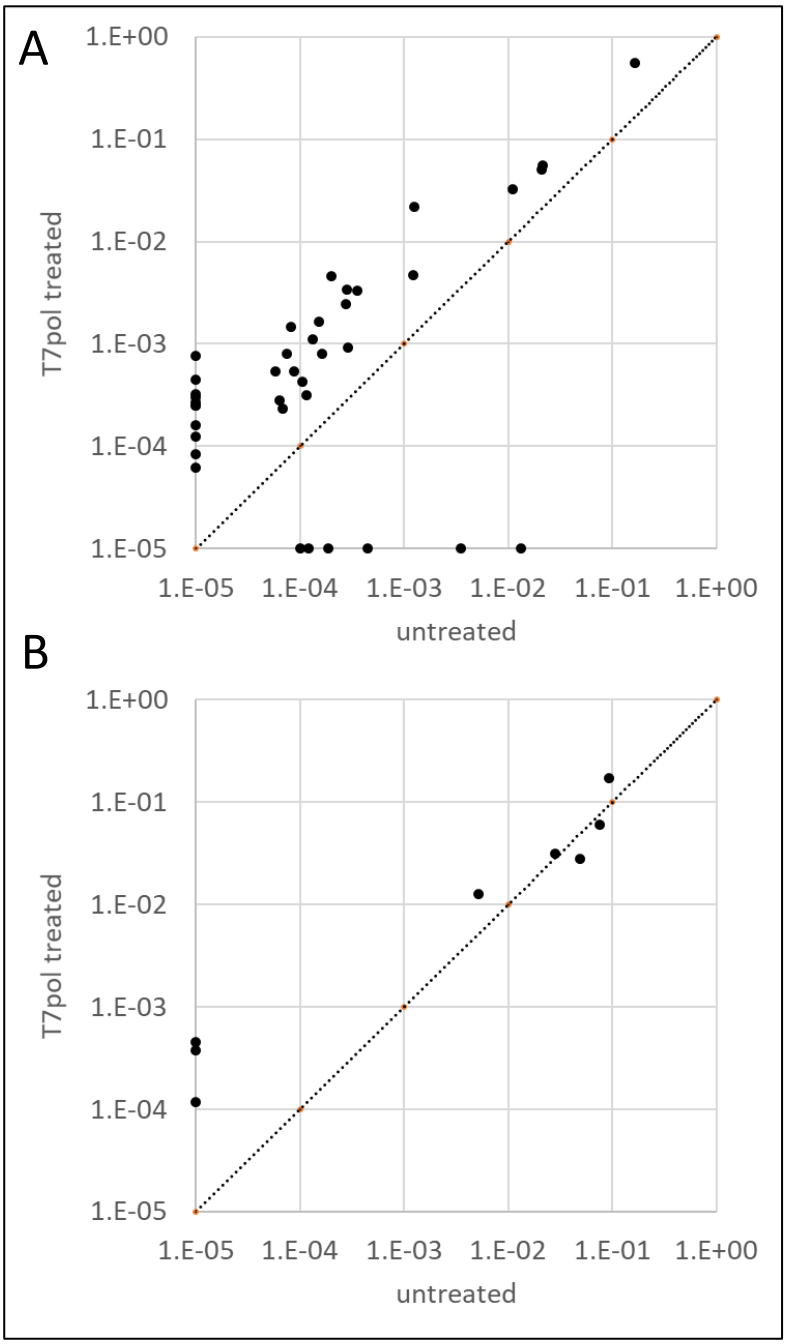

Figure 4: Relative abundance of each *Microviridae* detected in samples S4 (panel A) and S18 (panel B). Each dot represents one contig, with its abundance relative to all phages of the sample when sequenced without prior treatment for ssDNA (X axis) or after T7pol treatment (Y axis). The dotted line shows the bisector. Contigs undetected with one of the treatments were assigned an artificial value of 10^{-5}.

425

426 ***Discussion***

427 In the present benchmarking experiment, xGen libraries performed on untreated sonicated DNA were
428 the most detrimental to ssDNA sequencing: ssDNA was recovered at levels 10 to over 30-fold less than
429 expected. A previous study that also used synthetic mixes to compare MDA and xGen methods
430 concluded that ssDNA sequencing was quantitative with xGen libraries (Roux et al., 2016). Many subtle
431 differences might have led to the different conclusions. First, in this previous report, phage
432 concentrations were estimated by epifluorescence, a method that might have underestimated the two
433 *Microviridae* phage concentrations (PhiX174 and Alp3), as these particles are particularly dim under
434 the microscope. Second, the kit used for DNA extraction (QIAamp DNA Mini Kit) was said to recover
435 only 27% of the DNA for dsDNA phages while providing full recovery of ssDNA phages, so that
436 proportions of dsDNA phages were artificially inflated *a posteriori*. In the present work, a phenol–
437 chloroform extraction protocol was used, and no *a posteriori* corrections were made. Third, we found
438 that ssDNA was more sensitive to shearing during the sonication step, and the parameters are likely to
439 vary between sonication procedures. Fourth, we showed that some ssDNA was lost in our protocol at
440 the magnetic bead step after sonication (the details of library preparation are not mentioned in (Roux
441 et al., 2016). Clearly, all steps of DNA treatments should be carefully tested to ensure proper recovery
442 of ssDNA. Nevertheless, our observation confirms the notion that pretreatments permitting the
443 conversion of all ssDNA molecules to dsDNA prior to sonication should limit downstream bias, such as
444 those we observed here. Having all DNA in the dsDNA state at the onset of library preparation also
445 permits more accurate DNA concentration measurements, which is key for the tuning of sonication
446 parameters, according to each kit supplier's instructions.

447 Historically, MDA was the first method used to convert ssDNA to dsDNA; however, this method has
448 long been known to be detrimental for the quantitative assessment of viromes containing a mix of ss-
449 and dsDNA genomes (Kim and Bae, 2011; Roux et al., 2016). The standard 90-120 minute incubation
450 time used for MDA was reported to amplify ssDNA by an excess of 33 to 44-fold when the input ssDNA
451 was 2% (Roux et al., 2016). We found, however, that a shortening of the incubation time to 30 minutes
452 (designated here "sMDA") somewhat reduces the bias favoring ssDNA genomes: they were only in 8.6-
453 fold excess when starting from 5.9% input ssDNA. However, starting with 48.4% ssDNA led to final
454 ssDNA proportion of 98% of all sequenced DNA, somehow hiding all remaining dsDNA phage content.

455 T7pol pretreatment appears to be a better method than sMDA for sequencing DNA viromes. The
456 overall distance between the final sequencing product and the input DNA was the least in this case, as
457 well as being the most consistent for the two tested compositions. In particular, with respect to ssDNA,
458 the final ssDNA genome proportions were only slightly lower than input ssDNA when the input phage
459 mix had a high proportion of ssDNA (48.4%). However, for the low input ssDNA mix, the final
460 proportion was 8.2-fold lower than expected. It may be that the annealing step required for T7pol-
461 mediated DNA replication is less efficient when the ssDNA molecules are a minority within a complex
462 sample. More work is needed to improve further the T7pol treatment. In fact, the optimal
463 concentration of degenerated 20-mer oligonucleotides was very high (10µM), and even at this high
464 level, only a minor fraction of these 20-mers are predicted to anneal perfectly with the template. We
465 surmise that using shorter degenerated primers (such as 10-mer or 15-mer, instead of 20-mer) may
466 function as well, and with lower overall primer concentrations. With the T7pol treatment, we also
467 observed an improvement in the detection of *Microviridae*, which have ssDNA genomes, in two human
468 fecal viromes sequenced with xGen libraries. This shows that such a treatment is feasible on natural
469 samples and reinforces the interest in such a method.

470 It should be noted, however, that none of the protocols tested allowed the generation of an accurate
471 image of the relative proportions of the five input phages of the two synthetic communities. This
472 should be kept in mind when applying ecological metrics such as diversity and richness to viral

473 metagenomics data. Compared to bacterial metagenomics, ecological analysis based on viral
474 metagenomics is still in its infancy.

475 The T7pol pretreatment adds only a marginal cost (~1 euro per sample) to the library preparations
476 compared to a Genomiphi MDA pretreatment (20 euros per sample). Moreover, it should be possible
477 to apply it to samples planned for any kind of downstream library preparation kit for low DNA amounts,
478 such as the Nextera or TruSeq DNA nano kits from Illumina, making it independent of the 25% more
479 expensive xGen kit, which was used here for comparison purposes. Further analyses are needed to
480 explore this possibility.

481 Furthermore, the T7pol method described here might be a useful addition in the future, for projects
482 aiming at simultaneously describing the bacterial and viral components of their microbial ecosystems
483 without missing ssDNA viruses. In fact, several large databases of phage contigs have already been
484 generated thanks to the data mining of shotgun metagenomics (Camarillo-Guerrero et al., 2021;
485 Gregory et al., 2020; Nayfach et al., 2021b; Tisza et al., 2021). Such studies rely on the sorting of viral
486 contigs among all other microbial contigs based on their characteristics and gene contents (Guo et al.,
487 2021; Kieft et al., 2020). While this method is certainly efficient in detecting prophages, as well as
488 phage DNA replicating inside bacteria and possibly encapsidated DNA, ssDNA phage genomes will
489 probably escape analysis, as no pretreatment step ensuring their conversion into dsDNA is performed
490 at present (Camarillo-Guerrero et al., 2021; Nayfach et al., 2021b; Tisza et al., 2021). We noted,
491 however, that *Microviridae* were sometimes present in studies assembling viral sequences from such
492 shotgun metagenomic samples which, in theory, should not have sequenced ssDNA (Camarillo-
493 Guerrero et al., 2021; Nayfach et al., 2021b; Tisza et al., 2021). This might be explained if dsDNA
494 replication intermediates were extracted together with bacterial DNA. We cannot exclude, however,
495 that, depending on the biochemistry of each library preparation kit, the ssDNA fraction might be
496 included unknowingly, and sequenced quantitatively. In any case, the present work shows that adding
497 a T7 polymerase pretreatment can improve the sequencing of ssDNA viruses.

498

499 ***Conclusion:*** We conclude that T7pol pretreatment is a better alternative to MDA for the shotgun
500 sequencing of both the dsDNA and ssDNA fractions of viromes, which is easy to implement and
501 inexpensive.

502 ***Declarations***

503 *Ethics approval and consent to participate.* Approval for human studies was obtained from the local
504 ethics committee (Comité de Protection des Personnes Ile-de-France IV, IRB 00003835 Suivitheque
505 study; registration number 2012/05NICB).

506 *Consent for publication.* Not applicable

507 *Availability of data and material*: The supplementary material (containing all supplementary figures
508 and tables), as well as the raw reads generated for this study are available at
509 https://doi.org/10.57745/C0BAPR.

510 *Competing interests:* The authors declare they have no competing interests.

511 *Funding:* This work was funded by INRAE and Sorbonne Université, as well as the ANR project
512 PRIMAVERA.

513 *Authors' contributions:* MB, IT, QLB and FL conceived and realized the experiments, analyzed the data
514 and contributed to the redaction of the manuscript. MAP supervised the research and wrote the

manuscript. MDP and LDS supervised the research and contributed to the redaction of the manuscript. SAS contributed to the statistical analysis of the data and to the redaction of the manuscript.

Acknowledgments: The Migale platform at INRAE, on which bioinformatics analyses were conducted, is warmly thanked for its constant support and help.

References

Aitchison, J. (1982). The Statistical Analysis of Compositional Data. Journal of the Royal Statistical Society Series B (Methodological) *44*, 139-177.

Bin Jang, H., Bolduc, B., Zablocki, O., Kuhn, J.H., Roux, S., Adriaenssens, E.M., Brister, J.R., Kropinski, A.M., Krupovic, M., Lavigne, R.*, et al.* (2019). Taxonomic assignment of uncultivated prokaryotic virus genomes is enabled by gene-sharing networks. Nat Biotechnol *37*, 632-639.

Blanco, L., Bernad, A., Lazaro, J.M., Martin, G., Garmendia, C., and Salas, M. (1989). Highly efficient DNA synthesis by the phage phi 29 DNA polymerase. Symmetrical mode of DNA replication. J Biol Chem *264*, 8935-8940.

Camarillo-Guerrero, L.F., Almeida, A., Rangel-Pineros, G., Finn, R.D., and Lawley, T.D. (2021). Massive expansion of human gut bacteriophage diversity. Cell *184*, 1098-1109 e1099.

Canceill, D., Viguera, E., and Ehrlich, S.D. (1999). Replication slippage of different DNA polymerases is inversely related to their strand displacement efficiency. J Biol Chem *274*, 27481-27490.

Castro-Mejia, J.L., Muhammed, M.K., Kot, W., Neve, H., Franz, C.M., Hansen, L.H., Vogensen, F.K., and Nielsen, D.S. (2015). Optimizing protocols for extraction of bacteriophages prior to metagenomic analyses of phage communities in the human gut. Microbiome *3*, 64.

Chen, S., Zhou, Y., Chen, Y., and Gu, J. (2018). fastp: an ultra-fast all-in-one FASTQ preprocessor. Bioinformatics *34*, i884-i890.

Cook, R., Brown, N., Redgwell, T., Rihtman, B., Barnes, M., Clokie, M., Stekel, D.J., Hobman, J., Jones, M.A., and Millard, A. (2021). INfrastructure for a PHAge REference Database: Identification of Large-Scale Biases in the Current Collection of Cultured Phage Genomes. Phage (New Rochelle) *2*, 214-223.

De Paepe, M., De Monte, S., Robert, L., Lindner, A.B., and Taddei, F. (2010). Emergence of variability in isogenic Escherichia coli populations infected by a filamentous virus. PLoS One *5*, e11823.

Deng, L., Silins, R., Castro-Mejia, J.L., Kot, W., Jessen, L., Thorsen, J., Shah, S., Stokholm, J., Bisgaard, H., Moineau, S.*, et al.* (2019). A Protocol for Extraction of Infective Viromes Suitable for Metagenomics Sequencing from Low Volume Fecal Samples. Viruses *11*.

Feige, U., and Stirm, S. (1976). On the structure of the Escherichia coli C cell wall lipopolysaccharide core and on its phiX174 receptor region. Biochem Biophys Res Commun *71*, 566-573.

González-Cansino, J.L., Vieyra-Eusebio, M.T., Vera-Robles, L.I., and Hernández-Arana, A. (2019). Environmental adjustments of the cooperativity in M13 phage thermal denaturation. Thermochimica Acta *672*, 53-59.

Gregory, A.C., Zablocki, O., Zayed, A.A., Howell, A., Bolduc, B., and Sullivan, M.B. (2020). The Gut Virome Database Reveals Age-Dependent Patterns of Virome Diversity in the Human Gut. Cell Host Microbe *28*, 724-740 e728.

Guo, J., Bolduc, B., Zayed, A.A., Varsani, A., Dominguez-Huerta, G., Delmont, T.O., Pratama, A.A., Gazitua, M.C., Vik, D., Sullivan, M.B.*, et al.* (2021). VirSorter2: a multi-classifier, expert-guided approach to detect diverse DNA and RNA viruses. Microbiome *9*, 37.

Hernandez, A.J., Lee, S.J., and Richardson, C.C. (2016). Primer release is the rate-limiting event in lagging-strand synthesis mediated by the T7 replisome. Proc Natl Acad Sci U S A *113*, 5916-5921.

Hsieh, S.Y., Tariq, M.A., Telatin, A., Ansorge, R., Adriaenssens, E.M., Savva, G.M., Booth, C., Wileman, T., Hoyles, L., and Carding, S.R. (2021). Comparison of PCR versus PCR-Free DNA Library Preparation for Characterising the Human Faecal Virome. Viruses *13*.

Hyatt, D., Chen, G.L., Locascio, P.F., Land, M.L., Larimer, F.W., and Hauser, L.J. (2010). Prodigal: prokaryotic gene recognition and translation initiation site identification. BMC Bioinformatics *11*, 119.

Kent, W.J. (2002). BLAT--the BLAST-like alignment tool. Genome Res *12*, 656-664.

Kieft, K., Zhou, Z., and Anantharaman, K. (2020). VIBRANT: automated recovery, annotation and curation of microbial viruses, and evaluation of viral community function from genomic sequences. Microbiome *8*, 90.

Kim, K.H., and Bae, J.W. (2011). Amplification methods bias metagenomic libraries of uncultured single-stranded and double-stranded DNA viruses. Appl Environ Microbiol *77*, 7663-7668.

568 Langmead, B., and Salzberg, S.L. (2012). Fast gapped-read alignment with Bowtie 2. Nat Methods *9*,
569 357-359.
570 Lechner, R.L., and Richardson, C.C. (1983). A preformed, topologically stable replication fork.
571 Characterization of leading strand DNA synthesis catalyzed by T7 DNA polymerase and T7 gene 4
572 protein. J Biol Chem *258*, 11185-11196.
573 Li, H., and Durbin, R. (2009). Fast and accurate short read alignment with Burrows-Wheeler transform.
574 Bioinformatics *25*, 1754-1760.
575 McMurdie, P.J., and Holmes, S. (2013). phyloseq: an R package for reproducible interactive analysis
576 and graphics of microbiome census data. PLoS One *8*, e61217.
577 Nayfach, S., Camargo, A.P., Schulz, F., Eloe-Fadrosh, E., Roux, S., and Kyrpides, N.C. (2021a). CheckV
578 assesses the quality and completeness of metagenome-assembled viral genomes. Nat Biotechnol *39*,
579 578-585.
580 Nayfach, S., Paez-Espino, D., Call, L., Low, S.J., Sberro, H., Ivanova, N.N., Proal, A.D., Fischbach, M.A.,
581 Bhatt, A.S., Hugenholtz, P.*, et al.* (2021b). Metagenomic compendium of 189,680 DNA viruses from the
582 human gut microbiome. Nat Microbiol *6*, 960-970.
583 Pandolfo, M., Telatin, A., Lazzari, G., Adriaenssens, E.M., and Vitulo, N. (2022). MetaPhage: an
584 Automated Pipeline for Analyzing, Annotating, and Classifying Bacteriophages in Metagenomics
585 Sequencing Data. mSystems *7*, e0074122.
586 Prjibelski, A., Antipov, D., Meleshko, D., Lapidus, A., and Korobeynikov, A. (2020). Using SPAdes De
587 Novo Assembler. Curr Protoc Bioinformatics *70*, e102.
588 Roux, S., Solonenko, N.E., Dang, V.T., Poulos, B.T., Schwenck, S.M., Goldsmith, D.B., Coleman, M.L.,
589 Breitbart, M., and Sullivan, M.B. (2016). Towards quantitative viromics for both double-stranded and
590 single-stranded DNA viruses. PeerJ *4*, e2777.
591 Sausset, R., Krupova, Z., Guédon, E., Peron, S., Grangier, A., Petit, M.-A., De Sordi, L., and De Paepe, M.
592 (2022). Comparison of interferometric light microscopy with nanoparticle tracking analysis for the
593 study of extracellular vesicles and bacteriophages. Journal of Extracellular Vesicles.
594 Shah, S.A., Deng, L., Thorsen, J., Pedersen, A.G., Dion, M.B., Castro-Mejia, J.L., Silins, R., Romme, F.O.,
595 Sausset, R., Jessen, L.E.*, et al.* (2023). Expanding known viral diversity in the healthy infant gut. Nat
596 Microbiol.
597 Shkoporov, A.N., Ryan, F.J., Draper, L.A., Forde, A., Stockdale, S.R., Daly, K.M., McDonnell, S.A., Nolan,
598 J.A., Sutton, T.D.S., Dalmasso, M.*, et al.* (2018). Reproducible protocols for metagenomic analysis of
599 human faecal phageomes. Microbiome *6*, 68.
600 Soding, J. (2005). Protein homology detection by HMM-HMM comparison. Bioinformatics *21*, 951-960.
601 Terzian, P., Olo Ndela, E., Galiez, C., Lossouarn, J., Perez Bucio, R.E., Mom, R., Toussaint, A., Petit, M.A.,
602 and Enault, F. (2021). PHROG: families of prokaryotic virus proteins clustered using remote homology.
603 NAR Genom Bioinform *3*, lqab067.
604 Tisza, M.J., Belford, A.K., Dominguez-Huerta, G., Bolduc, B., and Buck, C.B. (2021). Cenote-Taker 2
605 democratizes virus discovery and sequence annotation. Virus Evol *7*, veaa100.
606 Vasimuddin, M., Misra, S., Li, H., and Aluru, S. (2019). Efficient architecture-awar acceleration of BWA-
607 MEM for multi-core systems. Paper presented at: IEEE International parallel and distributed processing
608 symposium (IPDPS) (Rio de Janeiro, Brazil).
609 Wang, G., Li, S., Yan, Q., Guo, R., Zhang, Y., Chen, F., Tian, X., Lv, Q., Jin, H., Ma, X.*, et al.* (2022).
610 Optimization and evaluation of viral metagenomic amplification and sequencing procedures toward a
611 genome-level resolution of the human fecal DNA virome. J Adv Res.
612 Yilmaz, S., Allgaier, M., and Hugenholtz, P. (2010). Multiple displacement amplification compromises
613 quantitative analysis of metagenomes. Nat Methods *7*, 943-944.

614 Supplementary table 1: ssDNA concentrations (ng/µL), tested by two different methods

	Nanodrop		Qubit	
	measure 1	measure 2	measure 1	measure 2
ssDNA PhiX174 NEB, 100 ng/µL	101.6	95	76.2	67.6
ssDNA M13mp18 NEB, 25 ng/µL	18.8	18.5	15.7	15.4
Standard ssDNA of the Qubit kit, 20 ng/µL	23.8	23.1		

615

616 Supplementary table 2: Primers used for qPCR

Phage	Forward	Reverse	Reference
T4	ACTGGCCAGGTATTCGCA	ATGCTTCTTTAGCACCGGCA	[12]
lambda	GAGTGCGGAAGATGCAAAGG	TTAACAGTGCGTGACCAGG	[13]
SPP1	CGGGCTGAAATACCTGTGGA	TAGCCCCTCCTCCGATTGTT	[14]
PhiX174	GGTTCGTCAAGGACTGGTT	TTGAACAGCATCGGACTCAG	this work

617
618
619
620
621 Supplementary table 3: Synthetic mix preparations

Phage	initial stock	volume added for each mix (µL)		ratio of each phage	
	phage/mL	Mix high ssDNA	Mix low ssDNA	Mix high ssDNA	Mix low ssDNA
T4	3.3E+09	370.2	370.2	24.9%	30.1%
lambda	7.5E+10	16.5	32.9	25.2%	60.8%
SPP1	5.4E+09	13.2	23.7	1.5%	3.2%
phiX174	4.7E+09	32.1	32.1 (dil 10x)	3.1%	0.4%
M13-yfp	3.0E+10	73.8	73.8 (dil 10x)	45.3%	5.5%

622

623 Supplementary table 4: Proportion of the five genomes in input mixes and after sequencing, using the
624 different protocols. A panel, high ssDNA mix, B panel, low ssDNA mix.

A. high ssDNA mix	input	short MDA 1	short MDA 2	T7pol 1	T7pol 2	xGen without pretreatment 1	xGen without pretreatment 2
T4 (ds)	24.9%	1.2%	1.0%	54.8%	53.6%	81.4%	81.4%
Lambda (ds)	25.2%	0.8%	0.9%	13.4%	2.9%	16.2%	16.2%
SPP1 (ds)	1.5%	0.0%	0.0%	0.5%	0.7%	0.6%	0.6%
PhiX174 (ss)	3.1%	4.7%	5.1%	2.6%	2.5%	0.2%	0.1%
M13-yfp (ss)	45.3%	93.3%	92.9%	28.6%	40.2%	1.7%	1.7%
%ssDNA, in total	48.4%	98.0%	98.0%	31.3%	42.7%	1.9%	1.8%

625

B. low ssDNA mix	input	short MDA 1	short MDA 2	T7pol 1	T7pol 2	xGen without pretreatment 1	xGen without pretreatment 2
T4 (ds)	30.1%	23.3%	22.2%	65.3%	66.5%	68.1%	69.7%

Lambda (ds)	60.8%	27.5%	24.9%	33.1%	31.9%	31.0%	29.5%
SPP1 (ds)	3.2%	1.0%	1.0%	1.0%	1.0%	0.9%	0.7%
PhiX174 (ss)	0.4%	9.8%	11.4%	0.2%	0.1%	0.00%	0.00%
M13-yfp (ss)	5.5%	38.4%	40.3%	0.5%	0.6%	0.00%	0.09%
%ssDNA, in total	5.9%	48.2%	51.7%	0.7%	0.7%	0.0%	0.1%

Supplementary table 5: properties of the 4 assembled viromes

	Raw reads (number of pairs)	**Clean, non-human reads (number of pairs)**	**Number of present viral contigs**
S4_Raw	3 944 094	3 101 396	645
S4_T7Pol	2 654 472	2 016 857	702
S18_Raw	47 423 047	36 124 946	269
S18_T7Pol	6 266 796	5 331 092	181

629 Supplementary table 6: properties of the microviruses found in samples S4 and S18.

Contig	CheckV Quality	Length	GC%	Closer Relative	HostGenus
Microvirus_01	High-quality	5816	47.54	Human gut gokushovirus	NA
Microvirus_02	Medium-quality	4309	38.8	NA	Prevotella
Microvirus_03	Medium-quality	4289	38.7	NA	Prevotella
Microvirus_04	Complete	5961	43.9	Microviridae sp.	Faecalibacterium
Microvirus_05	Complete	5454	44.98	Sigmofec virus UA08Rod_5824	NA
Microvirus_06	Complete	7094	36.31	Microvirus sp.	Prevotella
Microvirus_07	Complete	5880	43.59	Poophage MBI-2016a	NA
Microvirus_08	Medium-quality	3185	36.17	NA	NA
Microvirus_09	High-quality	6650	40.33	Dipodfec virus UOA04_Rod_446	NA
Microvirus_10	High-quality	5925	44.1	Dipodfec virus UOA04_Rod_841	NA
Microvirus_11	Complete	6229	40.78	Microviridae sp.	Phocaeicola
Microvirus_12	Complete	6516	41.9	Microviridae sp.	NA
Microvirus_13	Complete	5845	47.44	NA	Alistipes
Microvirus_14	Complete	5063	43.33	Gokushovirinae sp.	NA
Microvirus_15	Medium-quality	3198	36.59	NA	NA
Microvirus_16	Complete	4891	42.32	Capybara microvirus Cap1_SP_263	NA
Microvirus_17	Complete	6300	38.59	Microviridae sp.	Bacteroides
Microvirus_18	Complete	5873	45.79	Gokushovirus WZ-2015a	Faecalibacterium
Microvirus_19	Complete	5847	43.66	Gokushovirus WZ-2015a	NA
Microvirus_20	Complete	5758	43.4	Gokushovirus WZ-2015a	Faecalibacterium
Microvirus_21	Complete	6720	37.35	Dipodfec virus UOA04_Rod_499	NA
Microvirus_22	Medium-quality	2631	43.18	NA	NA
Microvirus_23	Complete	6037	37.22	Microvirus sp.	NA
Microvirus_24	Complete	6123	35.72	Microvirus sp.	NA
Microvirus_25	High-quality	6775	38.79	Microvirus sp.	Prevotella
Microvirus_26	Complete	4800	45.02	Human gut gokushovirus	NA
Microvirus_27	Low-quality	2125	41.88	Gokushovirus WZ-2015a	NA
Microvirus_28	High-quality	5711	35.95	Microvirus sp.	NA
Microvirus_29	Medium-quality	3568	47.76	Human gut gokushovirus	NA
Microvirus_30	Complete	6963	38.33	Human gut microviridae SH-CHD8	NA
Microvirus_31	Complete	5168	44.54	Microviridae sp.	NA
Microvirus_32	Complete	5176	41	Gokushovirus WZ-2015a	NA
Microvirus_33	Complete	5499	46.79	Dipodfec virus UOA04_Rod_999	Alistipes_A
Microvirus_34	High-quality	5875	45.28	Gokushovirus WZ-2015a	Faecalibacterium
Microvirus_35	Complete	5335	45.74	NA	NA
Microvirus_36	Complete	5536	44.09	Microviridae sp.	Dysosmobacter
Microvirus_37	Medium-quality	3381	38.15	Tortoise microvirus 14	NA
Microvirus_38	Medium-quality	3042	35.77	Gokushovirinae sp.	NA
Microvirus_39	Medium-quality	2986	47.56	Gokushovirus WZ-2015a	NA
Microvirus_40	Complete	5919	45.65	Gokushovirus WZ-2015a	Faecalibacterium
Microvirus_41	Complete	5934	45.8	NA	NA
Microvirus_42	Complete	6619	37.68	Tortoise microvirus 1	NA
Microvirus_43	Complete	5157	41.09	Microviridae sp.	NA
Microvirus_44	Complete	5874	43.65	Gokushovirus WZ-2015a	Faecalibacterium

630

631 Supplementary table 7: Relative abundance (rel) of each microviral contig in samples S4 and S18 before
632 ("raw" column) and after T7pol treatment ("T7pol column").

Sample S4	S4_raw, rel	S4_T7pol, rel	Fold increase
Microvirus_01	1.67E-01	5.53E-01	3.32
Microvirus_02	2.16E-02	5.57E-02	2.58
Microvirus_03	2.11E-02	5.08E-02	2.41
Microvirus_04	1.10E-02	3.24E-02	2.95
Microvirus_05	1.25E-03	2.18E-02	17.47
Microvirus_06	1.31E-02	0	
Microvirus_07	1.21E-03	4.69E-03	3.88
Microvirus_08	1.99E-04	4.59E-03	23.10
Microvirus_09	3.52E-04	3.35E-03	9.52
Microvirus_10	2.82E-04	3.39E-03	12.03
Microvirus_11	3.48E-03	0	
Microvirus_12	2.74E-04	2.47E-03	9.02
Microvirus_13	1.54E-04	1.66E-03	10.81
Microvirus_14	8.25E-05	1.46E-03	17.72
Microvirus_15	1.32E-04	1.10E-03	8.37
Microvirus_16	2.90E-04	9.19E-04	3.17
Microvirus_17	1.65E-04	8.01E-04	4.86
Microvirus_18	7.54E-05	7.94E-04	10.53
Microvirus_19	0	7.65E-04	
Microvirus_20	8.79E-05	5.39E-04	6.13
Microvirus_21	5.84E-05	5.33E-04	9.14
Microvirus_22	1.06E-04	4.28E-04	4.05
Microvirus_23	4.46E-04	0	
Microvirus_24	0	4.44E-04	
Microvirus_25	1.16E-04	3.18E-04	2.75
Microvirus_26	6.33E-05	2.80E-04	4.42
Microvirus_27	0	3.26E-04	
Microvirus_28	6.87E-05	2.32E-04	3.38
Microvirus_29	0	2.98E-04	
Microvirus_30	0	2.65E-04	
Microvirus_31	0	2.50E-04	
Microvirus_32	0	2.50E-04	
Microvirus_33	1.89E-04	0	
Microvirus_34	0	0	
Microvirus_35	0	1.23E-04	
Microvirus_36	1.21E-04	0	
Microvirus_37	1.01E-04	0	
Microvirus_38	0	8.42E-05	
Microvirus_39	0	6.10E-05	
Richness	28	33	
Fold-increase (Average +/-standard deviation)			7.8 +/- 5.71
Sample S18	S18_raw, rel	S18_T7pol, rel	Fold increase
Microvirus_01	0	4.50E-04	
Microvirus_40	9.22E-02	1.70E-01	1.85
Microvirus_41	7.64E-02	5.99E-02	0.78
Microvirus_42	4.91E-02	2.78E-02	0.57
Microvirus_43	2.81E-02	3.11E-02	1.11
Microvirus_44	5.13E-03	1.27E-02	2.48
Microvirus_06	0	3.79E-04	
Microvirus_11	0	1.18E-04	
Richness	5	8	
Fold-increase (Average +/-standard deviation)			1.36 +/- 0.79

633 Supplementary table 8: Relative abundance (rel) of each microviral contig in samples S4 and S18 before
634 ("raw" column) and after T7pol treatment (“T7pol column”).

Contig name	S4_raw, rel	S4_T7pol, rel	Contig name	S18_raw, rel	S18_T7pol, rel
Caudoviricetes_01	9.72E-02	6.13E-02	Caudoviricetes_148	2.88E-01	1.74E-01
Caudoviricetes_02	6.70E-02	3.31E-02	Caudoviricetes_03	1.94E-01	2.49E-01
Caudoviricetes_03	4.35E-02	1.79E-02	Caudoviricetes_149	2.97E-02	1.45E-02
Caudoviricetes_04	2.16E-02	1.62E-02	Caudoviricetes_150	1.35E-02	1.12E-02
Caudoviricetes_05	2.04E-02	1.22E-02	Caudoviricetes_151	7.21E-03	7.82E-03
Caudoviricetes_06	1.80E-02	7.85E-03	Caudoviricetes_152	4.35E-03	4.49E-03
Caudoviricetes_07	2.06E-02	4.53E-03	Caudoviricetes_153	4.31E-03	3.37E-03
Caudoviricetes_08	2.14E-02	0	Caudoviricetes_154	2.19E-03	4.04E-03
Caudoviricetes_09	1.56E-02	1.18E-04	Caudoviricetes_155	2.68E-03	3.10E-03
Caudoviricetes_10	1.31E-02	2.47E-03	Caudoviricetes_156	2.26E-03	2.49E-03
Caudoviricetes_11	1.51E-02	0.00E+00	Caudoviricetes_157	2.21E-03	2.31E-03
Caudoviricetes_12	1.29E-02	2.82E-04	Caudoviricetes_158	2.28E-03	1.23E-03
Caudoviricetes_13	1.02E-02	2.50E-03	Caudoviricetes_159	1.53E-03	1.40E-03
Caudoviricetes_14	9.87E-03	2.39E-03	Caudoviricetes_160	1.03E-03	1.69E-03
Caudoviricetes_15	9.52E-03	2.65E-03	Caudoviricetes_161	9.80E-04	1.34E-03
Caudoviricetes_16	9.60E-03	2.41E-03	Caudoviricetes_162	6.30E-04	9.22E-04
Caudoviricetes_17	9.46E-03	2.28E-03	Caudoviricetes_163	7.34E-04	4.88E-04
Caudoviricetes_18	9.08E-03	2.29E-03	Caudoviricetes_164	3.09E-04	7.55E-04
Caudoviricetes_19	9.25E-03	2.02E-03	Caudoviricetes_165	5.87E-04	4.68E-04
Caudoviricetes_20	8.88E-03	2.15E-03	Caudoviricetes_08	0	9.05E-04
Caudoviricetes_21	7.00E-03	3.88E-03	Caudoviricetes_166	4.71E-04	4.10E-04
Caudoviricetes_22	7.28E-03	3.29E-03	Caudoviricetes_167	2.89E-04	5.81E-04
Caudoviricetes_23	8.56E-03	1.93E-03	Caudoviricetes_168	4.23E-04	4.18E-04
Caudoviricetes_24	8.63E-03	1.62E-03	Caudoviricetes_169	3.33E-04	4.35E-04
Caudoviricetes_25	6.48E-03	1.41E-03	Caudoviricetes_170	3.64E-04	3.36E-04
Caudoviricetes_26	6.87E-03	2.82E-04	Caudoviricetes_171	3.14E-04	3.58E-04
Caudoviricetes_27	6.75E-03	3.38E-04	Caudoviricetes_172	2.30E-04	4.35E-04
Caudoviricetes_28	6.38E-03	0	Caudoviricetes_173	2.63E-04	3.83E-04
Caudoviricetes_29	4.80E-03	1.24E-03	Caudoviricetes_174	3.18E-04	3.14E-04
Caudoviricetes_30	4.69E-03	1.03E-03	Caudoviricetes_175	2.61E-04	3.48E-04
Caudoviricetes_31	5.63E-03	0	Caudoviricetes_176	2.92E-04	3.15E-04
Caudoviricetes_32	5.62E-03	0	Caudoviricetes_177	2.31E-04	3.72E-04
Caudoviricetes_33	3.85E-03	7.24E-04	Caudoviricetes_178	2.54E-04	3.01E-04
Caudoviricetes_34	2.58E-03	1.50E-03	Caudoviricetes_179	2.60E-04	2.81E-04
Caudoviricetes_35	3.46E-03	0	Caudoviricetes_180	1.65E-04	3.65E-04
Caudoviricetes_36	1.74E-03	1.38E-03	Caudoviricetes_181	1.97E-04	3.33E-04
Caudoviricetes_37	2.23E-03	7.15E-04	Caudoviricetes_182	3.21E-04	2.02E-04
Caudoviricetes_38	2.66E-03	0	Caudoviricetes_183	1.23E-04	3.89E-04
Caudoviricetes_39	2.63E-03	0	Caudoviricetes_184	3.50E-04	1.60E-04
Caudoviricetes_40	2.05E-03	4.67E-04	Caudoviricetes_185	1.68E-04	3.42E-04
Caudoviricetes_41	2.36E-03	0	Caudoviricetes_186	1.93E-04	3.08E-04
Caudoviricetes_42	1.52E-03	8.06E-04	Caudoviricetes_187	2.97E-04	2.00E-04
Caudoviricetes_43	2.23E-03	0	Caudoviricetes_188	1.76E-04	3.18E-04

Caudoviricetes_44	2.17E-03	0	Caudoviricetes_09	0	4.88E-04
Caudoviricetes_45	2.15E-03	0	Caudoviricetes_189	3.44E-04	1.43E-04
Caudoviricetes_46	9.47E-04	7.54E-04	Caudoviricetes_11	0	4.82E-04
Caudoviricetes_47	1.69E-03	0	Caudoviricetes_190	3.37E-04	1.38E-04
Caudoviricetes_48	8.93E-04	7.49E-04	Caudoviricetes_191	2.23E-04	2.43E-04
Caudoviricetes_49	1.14E-03	3.89E-04	Caudoviricetes_192	3.00E-04	1.52E-04
Caudoviricetes_50	1.52E-03	0	Caudoviricetes_193	2.20E-04	2.30E-04
Caudoviricetes_51	9.71E-04	5.34E-04	Caudoviricetes_194	1.69E-04	2.70E-04
Caudoviricetes_52	1.34E-03	0	Caudoviricetes_195	2.83E-04	1.54E-04
Caudoviricetes_53	8.29E-04	4.72E-04	Caudoviricetes_196	2.19E-04	1.99E-04
Caudoviricetes_54	6.25E-04	6.66E-04	Caudoviricetes_197	1.80E-04	2.32E-04
Caudoviricetes_55	1.20E-03	0	Caudoviricetes_198	1.62E-04	2.41E-04
Caudoviricetes_56	1.01E-03	1.77E-04	Caudoviricetes_199	1.84E-04	2.13E-04
Caudoviricetes_57	1.03E-03	0	Caudoviricetes_200	2.34E-04	1.60E-04
Caudoviricetes_58	8.01E-04	2.05E-04	Caudoviricetes_201	1.54E-04	2.37E-04
Caudoviricetes_59	9.98E-04	0	Caudoviricetes_202	1.44E-04	2.39E-04
Caudoviricetes_60	8.26E-04	1.56E-04	Caudoviricetes_203	1.81E-04	1.98E-04
Caudoviricetes_61	9.52E-04	0	Caudoviricetes_204	1.96E-04	1.80E-04
Caudoviricetes_62	9.28E-04	0	Caudoviricetes_205	2.02E-04	1.62E-04
Caudoviricetes_63	6.60E-04	2.44E-04	Caudoviricetes_206	1.96E-04	1.62E-04
Caudoviricetes_64	8.32E-04	0	Caudoviricetes_12	0	3.53E-04
Caudoviricetes_65	5.15E-04	2.72E-04	Caudoviricetes_207	2.13E-04	1.40E-04
Caudoviricetes_66	4.85E-04	3.00E-04	Caudoviricetes_208	1.83E-04	1.64E-04
Caudoviricetes_67	4.75E-04	2.96E-04	Caudoviricetes_209	1.84E-04	1.61E-04
Caudoviricetes_68	7.45E-04	0	Caudoviricetes_210	1.72E-04	1.71E-04
Caudoviricetes_69	7.07E-04	0	Caudoviricetes_211	3.38E-04	0
Caudoviricetes_70	6.94E-04	0	Caudoviricetes_212	1.08E-04	2.27E-04
Caudoviricetes_71	3.86E-04	2.95E-04	Caudoviricetes_213	1.65E-04	1.65E-04
Caudoviricetes_72	6.28E-04	0	Caudoviricetes_214	1.51E-04	1.68E-04
Caudoviricetes_73	4.32E-04	1.68E-04	Caudoviricetes_215	1.84E-04	1.32E-04
Caudoviricetes_74	3.60E-04	2.32E-04	Caudoviricetes_216	1.49E-04	1.63E-04
Caudoviricetes_75	5.89E-04	0	Caudoviricetes_217	1.39E-04	1.72E-04
Caudoviricetes_76	4.07E-04	1.58E-04	Caudoviricetes_218	1.45E-04	1.66E-04
Caudoviricetes_77	5.33E-04	0	Caudoviricetes_219	1.27E-04	1.83E-04
Caudoviricetes_78	5.30E-04	0	Caudoviricetes_220	1.43E-04	1.56E-04
Caudoviricetes_79	5.29E-04	0	Caudoviricetes_221	2.90E-04	0
Caudoviricetes_80	2.98E-04	2.21E-04	Caudoviricetes_222	1.31E-04	1.57E-04
Caudoviricetes_81	3.32E-04	1.34E-04	Caudoviricetes_223	1.21E-04	1.66E-04
Caudoviricetes_82	2.68E-04	1.89E-04	Caudoviricetes_224	1.19E-04	1.68E-04
Caudoviricetes_83	2.48E-04	2.03E-04	Caudoviricetes_225	1.58E-04	1.21E-04
Caudoviricetes_84	3.58E-04	8.26E-05	Caudoviricetes_226	1.26E-04	1.52E-04
Caudoviricetes_85	4.14E-04	0	Caudoviricetes_227	1.50E-04	1.27E-04
Caudoviricetes_86	4.00E-04	0	Caudoviricetes_228	1.35E-04	1.35E-04
Caudoviricetes_87	3.76E-04	0	Caudoviricetes_28	0	2.67E-04
Caudoviricetes_88	3.75E-04	0	Caudoviricetes_229	1.37E-04	1.21E-04
Caudoviricetes_89	2.14E-04	1.61E-04	Caudoviricetes_230	9.24E-05	1.47E-04
Caudoviricetes_90	3.60E-04	0	Caudoviricetes_231	1.45E-04	8.69E-05

Caudoviricetes_91	1.40E-04	2.09E-04
Caudoviricetes_92	1.96E-04	1.31E-04
Caudoviricetes_93	1.93E-04	1.33E-04
Caudoviricetes_94	2.87E-04	0
Caudoviricetes_95	2.30E-04	4.04E-05
Caudoviricetes_96	2.66E-04	0
Caudoviricetes_97	2.52E-04	0
Caudoviricetes_98	2.47E-04	0
Caudoviricetes_99	1.19E-04	1.26E-04
Caudoviricetes_100	1.59E-04	7.98E-05
Caudoviricetes_101	2.35E-04	0
Caudoviricetes_102	2.30E-04	0
Caudoviricetes_103	1.73E-04	4.99E-05
Caudoviricetes_104	2.19E-04	0
Caudoviricetes_105	2.17E-04	0
Caudoviricetes_106	2.14E-04	0
Caudoviricetes_107	1.51E-04	5.07E-05
Caudoviricetes_108	1.31E-04	6.64E-05
Caudoviricetes_109	1.33E-04	5.48E-05
Caudoviricetes_110	1.04E-04	7.87E-05
Caudoviricetes_111	1.78E-04	0
Caudoviricetes_112	1.68E-04	0
Caudoviricetes_113	1.66E-04	0
Caudoviricetes_114	1.53E-04	0
Caudoviricetes_115	1.43E-04	0
Caudoviricetes_116	8.00E-05	6.25E-05
Caudoviricetes_117	1.42E-04	0
Caudoviricetes_118	1.40E-04	0
Caudoviricetes_119	9.09E-05	4.29E-05
Caudoviricetes_120	6.67E-05	5.28E-05
Caudoviricetes_121	1.10E-04	0
Caudoviricetes_122	1.06E-04	0
Caudoviricetes_123	4.95E-05	5.23E-05
Caudoviricetes_124	9.78E-05	0
Caudoviricetes_125	9.45E-05	0
Caudoviricetes_126	9.40E-05	0
Caudoviricetes_127	9.38E-05	0
Caudoviricetes_128	8.30E-05	0
Caudoviricetes_129	8.14E-05	0
Caudoviricetes_130	6.80E-05	0
Caudoviricetes_131	6.64E-05	0
Caudoviricetes_132	6.63E-05	0
Caudoviricetes_133	6.36E-05	0
Caudoviricetes_134	6.31E-05	0
Caudoviricetes_135	5.97E-05	0
Caudoviricetes_136	0	5.06E-05
Caudoviricetes_137	0	4.60E-05
Caudoviricetes_31	0	2.08E-04
Caudoviricetes_232	1.22E-04	8.48E-05
Caudoviricetes_233	1.04E-04	1.03E-04
Caudoviricetes_234	2.00E-04	0
Caudoviricetes_235	8.86E-05	1.09E-04
Caudoviricetes_32	0	1.92E-04
Caudoviricetes_236	1.87E-04	0
Caudoviricetes_237	1.71E-04	0
Caudoviricetes_238	1.69E-04	0
Caudoviricetes_39	0	1.58E-04
Caudoviricetes_239	1.51E-04	0
Caudoviricetes_27	0	1.40E-04
Caudoviricetes_35	0	1.38E-04
Caudoviricetes_240	0	1.36E-04
Caudoviricetes_26	0	1.35E-04
Caudoviricetes_241	1.23E-04	0
Caudoviricetes_242	0	1.22E-04
Caudoviricetes_243	1.13E-04	0
Caudoviricetes_244	1.10E-04	0
Caudoviricetes_245	0	1.10E-04
Caudoviricetes_246	0	1.06E-04
Caudoviricetes_247	0	9.79E-05
Caudoviricetes_248	0	9.20E-05
Caudoviricetes_43	0	8.68E-05
Caudoviricetes_249	0	7.20E-05
Caudoviricetes_250	1.93E-05	4.11E-05
Caudoviricetes_59	0	3.21E-05
Caudoviricetes_251	2.90E-05	0

Caudoviricetes_138	0	4.25E-05
Caudoviricetes_139	0	4.25E-05
Caudoviricetes_140	0	3.80E-05
Caudoviricetes_141	0	3.58E-05
Caudoviricetes_142	0	3.54E-05
Caudoviricetes_143	0	3.40E-05
Caudoviricetes_144	0	3.28E-05
Caudoviricetes_145	0	3.23E-05
Caudoviricetes_146	1.81E-05	0

637

638 Supplementary figure 1: pipeline of virome reads analysis

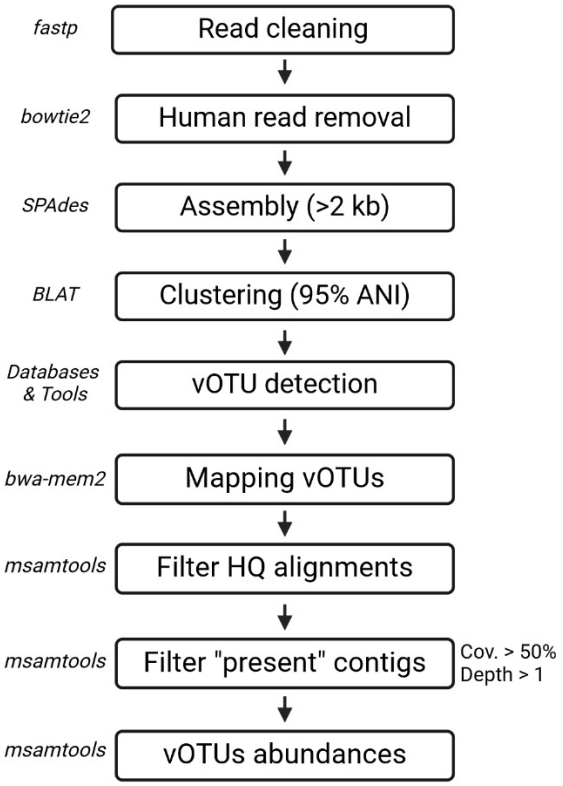

639

640

641 Supplementary figure 2: raw gel of figure 1

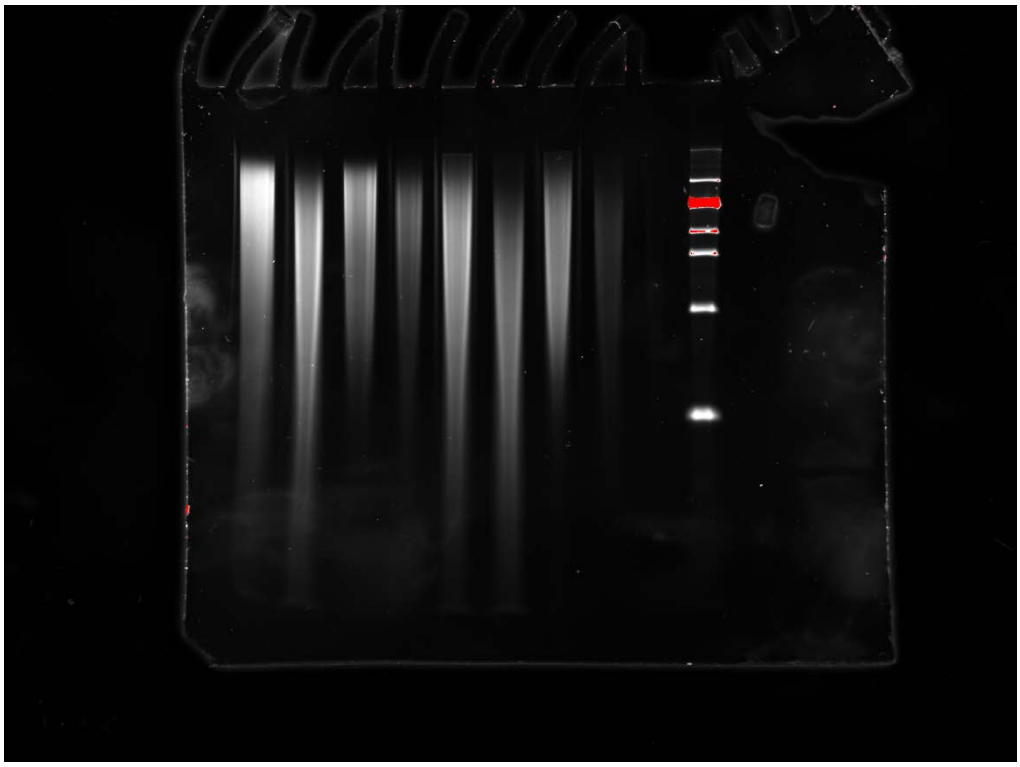

642

643 Supplementary figure 3: raw gel of figure 2.

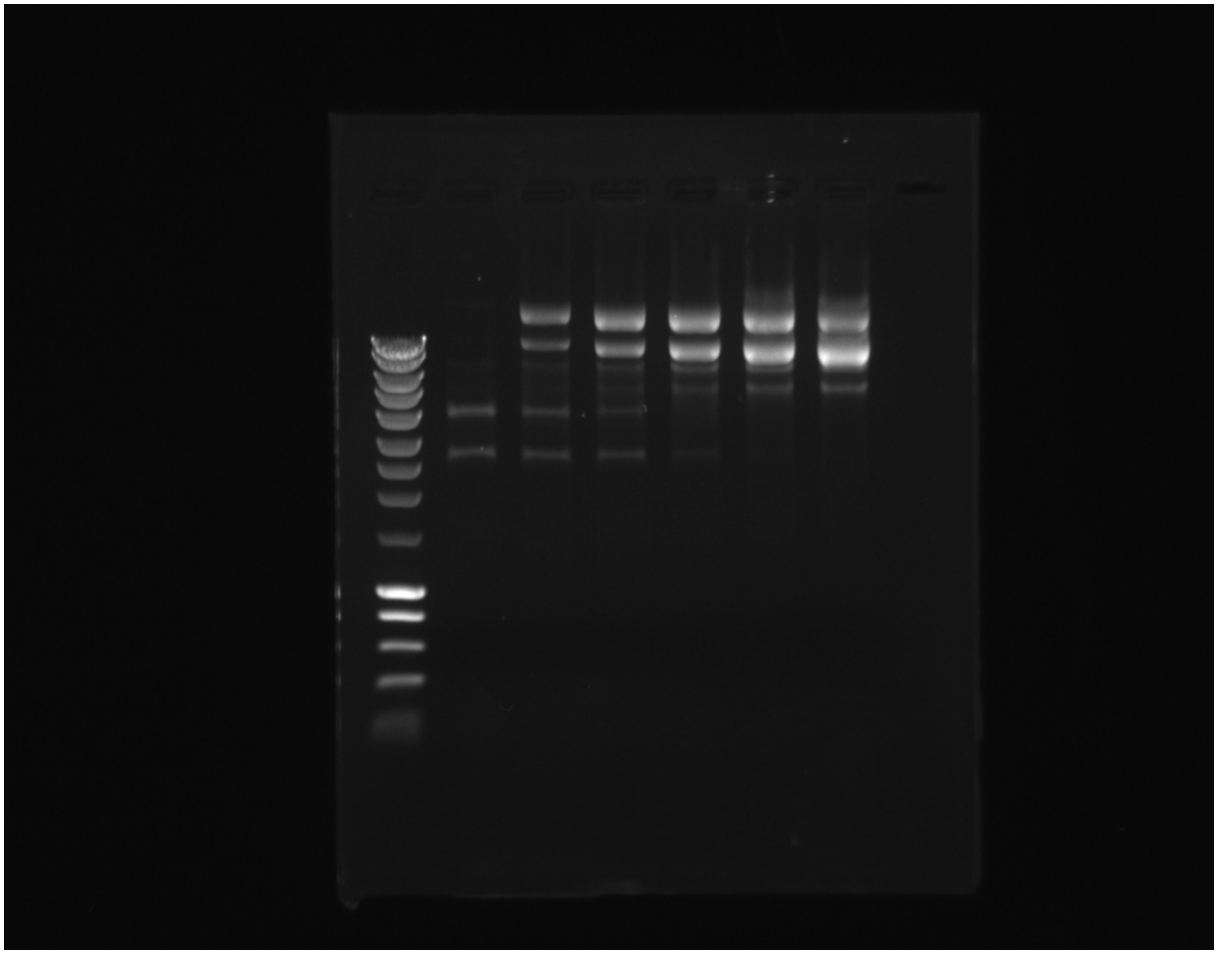

644

Supplementary figure 4: Relative abundance of each *Caudoviricetes* detected in samples S4 (top) and S18 (bottom). Each dot represents one contig, with its abundance relative to all phages of the sample when sequenced without prior treatment for ssDNA (X axis) or after T7pol treatment (Y axis). The dotted line shows the bisector. Contigs undetected with one of the treatments were assigned an artificial value of 10^{-5}.

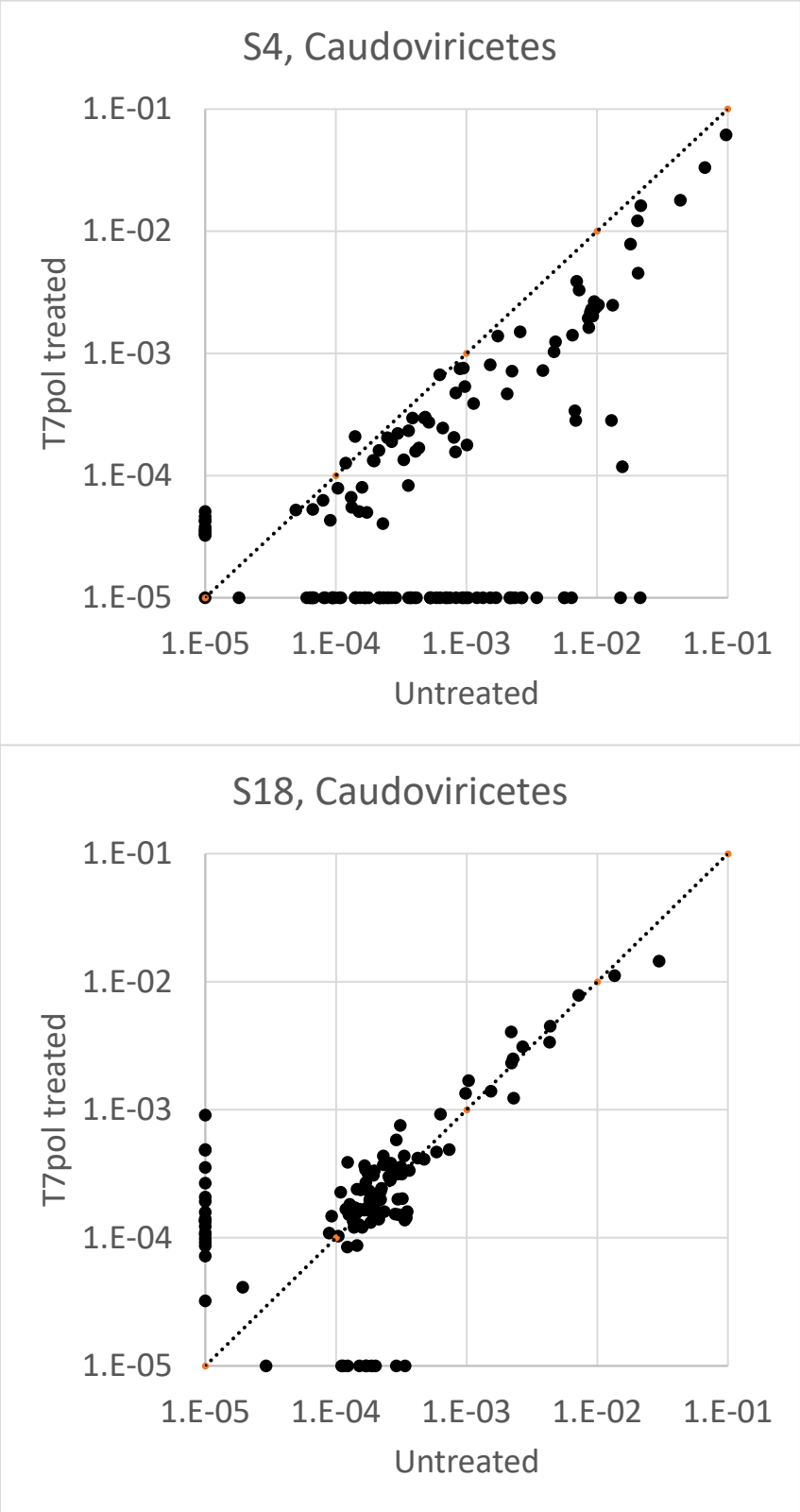

680 Supplementary figure 5: VipTree classification of the microviruses detected in samples S4 and S18.

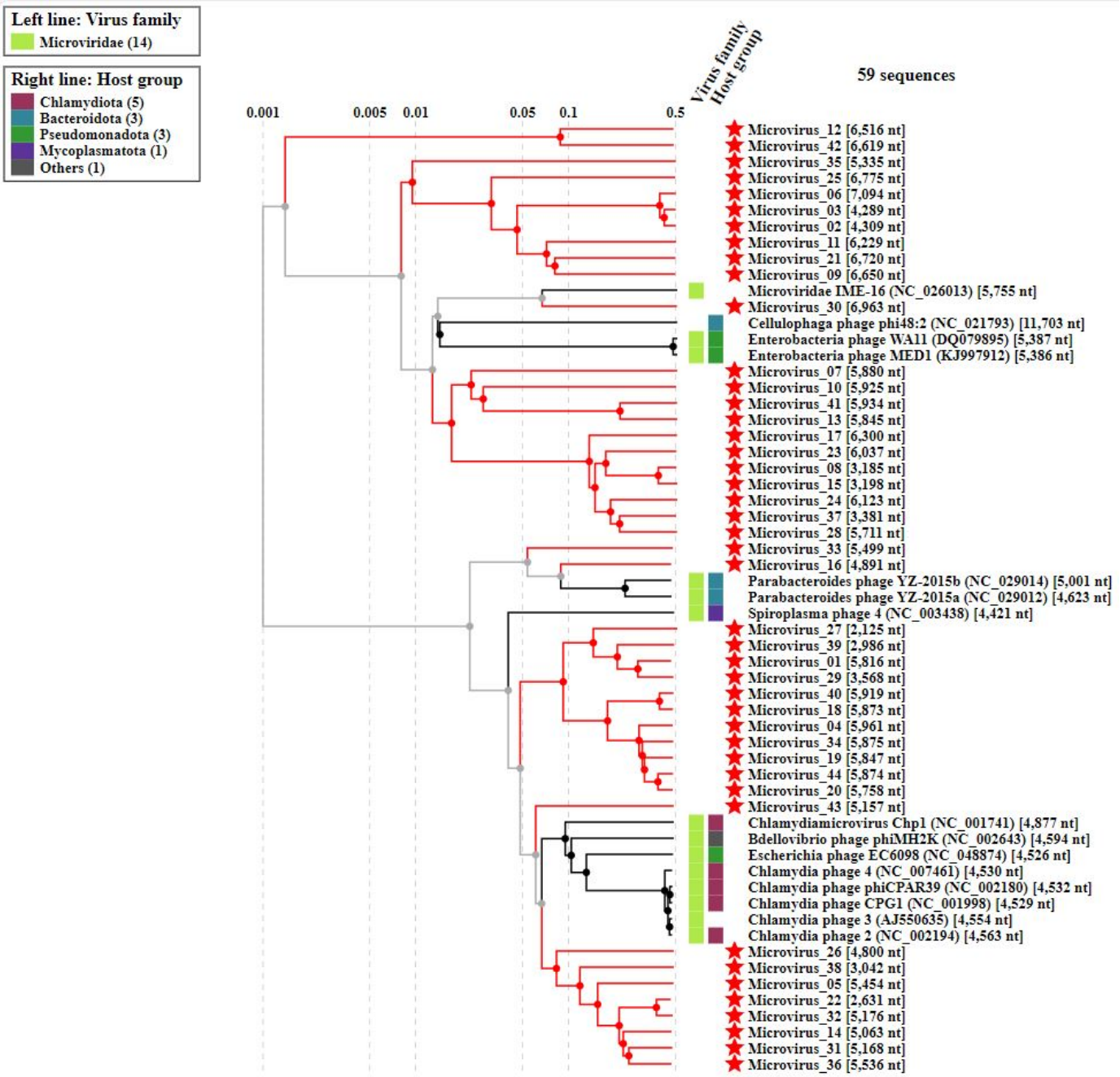

681